Radiative effects of ozone waves on the Northern Hemisphere polar vortex and its modulation by the QBO

Vered Silverman[1], Nili Harnik[1], Katja Matthes[2], Sandro W. Lubis[3], and Sebastian Wahl[2]

[1]Department of Geophysical, Atmospheric and Planetary Sciences, Tel Aviv University, Tel Aviv, Israel
[2]GEOMAR Helmholtz Centre for Ocean Research Kiel, Kiel, Germany
[3]Department of the Geophysical Sciences, The University of Chicago, USA

Correspondence to: Vered Silverman (veredsil@post.tau.ac.il)

Dear William Ward,

We thank the reviewers for their helpful comments which we think helped improve the manuscript. To address the issues raised we performed additional analysis of the ozone wave budget terms (see answer to comment #8 of reviewer #1) and calculated the statistical significance of the difference between the top and bottom panels of figure 4 (added in an appendix). We also modified the presentation by replacing figure 12 by a new one, adding figure A1, dividing the discussion of section 3 to 4 subsections, and rephrasing the paper throughout.

Reviewer #1

We thank the reviewer for reading the manuscript and providing their helpful comments. We address their issues below.

- Comment #1 – Page 3 lines 22-23: I'm not sure about the seasonality statement here. You should double check, but if I recall correctly, Watson and Gray (JAS 2014) find that the QBO signal is stronger later in the winter. This may be an important point in light of the fact that your argument hinges on the seasonal cycle of the waves and the mean. If I am correct here, it would be good for you to comment on how Watson and Gray's results apply to your study.

- Answer #1 - Watson and Gray (2014) indeed find a later Holton-Tan signal in their model, compared to our study and to ERA40, where it appears earlier in November. We note that Watson and Gray (2014) use the HadGEM2-CCS model, which is not coupled to chemistry, and it seems that zonally averaged ozone is used in the radiative scheme. Therefore, the lack of an early winter QBO response in their model is in actually in agreement with our results. We added this in the conclusions section. Thank you.

- Comment #2 – Page 4 lines 15-20: How does your approach deal with ozone flux convergences in the ZMO3 runs? While I understand that you only pass zonally symmetric ozone to the radiation code, the zonal mean ozone does still include one effect of ozone waves on the simulations if the zonal mean ozone field includes the flux convergences. You should

clarify this one way or the other and make it clear to readers exactly what pieces of wave ozone physics are included in each type of simulation (i.e. 3DO3 versus ZMO3).

- Answer #2- We intentionally keep the influence of ozone waves on the zonal mean ozone through advection, as we are interested only in the direct radiative effect of ozone which is the influence on Newtonian damping. We further clarified this on Page 4 line 25-26.

- Comment #3 – Page 30 line 30: You mention later that your results are robust to the 70th percentile choice, but I am wondering about the 100 hPa level. I say this because the 100 hPa level is a very sensitive region in the stratosphere as far as the "valving" of wave energy either upwards into the core of the vortex where the PV gradient is strong and there is a strong waveguide versus ducting the energy equatorward. I am guessing that your results are robust to this choice, but it would be good for readers to know this information. I say this mostly because I think your approach is novel and it would be good for readers to be able to have all of the information they need to apply the method in other contexts.

- Answer #3- We repeated the analysis for events chosen using the 50hPa level and the results are qualitatively similar (see Figures 1,2 below). We chose the 100hPa level since this is the region where the waves enter the stratosphere, and we wanted to identify the events before the wave changes the mean flow. This is mentioned briefly in the text on page 5 line 11-12.

- Comment #4 – Page 5 lines 14: Sorry to be picky, but I really think that you should include the original source here when discussing the inverse relationship between ozone and temperature, which is Craig and Ohring 1958, see citation below: http://journals.ametsoc.org/doi/abs/10.1175/1520-0469%281958%29015%3C0059%3ATTDOOR%3E2.0.CO%3B2 Also, while the Hartmann 1981 paper is nice in a qualitative sense, much more detailed information can be gathered from the following sets of papers that I think you should also cite: Nathan and Cordero JGR 2007, Hartmann and Garcia JAS 1979, and Garcia and Hartmann JAS 1980. I think in particular the Garcia references are important because they are directly relevant to the physical interpretations of your work and have a good amount of physical insight in them that readers should know about.

- Answer #4 - We replaced the reference to Craig and Ohring (1958), and thank the reviewer for this correction. We also added a sentence on why the ozone-temperature correlation is positive in the dynamically controlled region, with a reference to Hartmann and Garcia (1979) (page 6 line 5-6) and to Nathan and Cordero (2007) (page 6 line 18-19, page 13 line 21-25). Since this is not the topic of the paper, we decided not to elaborate any further.

- Comment #5 – Page 5 lines 10-30:Two related issues here. One, there is some seasonality to the ratio of advective to photochemical timescales and the ratio of advective to Newtonian cooling timescales (see Fig. 3 of Nathan and Cordero JGR 2007). Also, there is strong seasonality in regards to many wave properties as outlined carefully in Nathan and Li (JAS 1991) and Nathan and Cordero (JGR 2007). Do your results agree with these theoretical results? While this may not be a simple set of questions to answer, I think that lending some effort towards deciphering if your WACCM results

agree with previous theory would be nice. I will leave it up to you on where you want to comment on this (perhaps the results section is not the right place), but it would be helpful if you could comment somewhere in your text.

– Answer #5 - Nathan and Li (1991) showed that ozone wave effects are strongest in September, and weakest during January due to the large solar zenith angle. Also, when the waves peak in the lower stratosphere, where the ozone-temperature correlation is positive, the dominant ozone wave effect is to weaken the radiative damping in that region. This is indeed seen in September, where the temperature wave is stronger throughout the stratosphere in the 3DO3 run (we added a comment on this on page 6 line 30-32). On the other hand, when the waves penetrate higher into the upper stratosphere, where the ozone-temperature correlation is negative, the dominant wave radiative effect is to strengthen the thermal damping. As we show in Figure 3 - during September the wave peak is in the region where the ozone-temperature correlation is positive, thus the main effects are weaker wave damping, stronger waves (showed by the positive |T| anomalies), and correspondingly, a vertical displacement of the EP flux peak. In the WACCM model, it does not seem like this changes later in winter. Apart from the obvious model differences (1D vs CCM) it is possible this is also due to the limited height range (up to 2hPa) over which we zonally average the ozone field in the ZMO3 run in order to avoid large biases in the mesosphere. We added a comment to this effect on page 8 line 2-8.

– Comment #6 – Page 8 lines 25-30: Why are you using the beta-plane geometry form instead of the spherical form? I am wondering if your figure would look any different using the full form. I am also wondering a bit about your interpretation of the refractive index (RI) anomalies. In particular, while I do find your point regarding the ducting of wave energy in the middle portion of the domain (i.e. the blue region spanning 15-45 km in height and 70-80 N to 20 N) during west QBO, I am wondering about your interpretation during east QBO. That is, while there is a region of positive RI in the uppermost stratosphere during east QBO, before the wave energy gets there, it would first encounter the broad region of negative RI anomaly (i.e. the same blue region I just described above). And given that there appears to be a region of positive RI immediately underneath the blue region (i.e. the red region extending from 60 N to 30 N between 10-30 km in height), isn't it possible that a bunch of wave energy is also being ducted equatorward during east QBO (but lower than is being ducted during QBO west)? Indeed it is somewhat hard to tell from Fig. 8c, but it seems like there is additional EP-flux convergence near 30-40 N at 30 km for QBO east. I'm not saying that there is any inconsistency in your argument, but perhaps east QBO is characterized by both increased upper stratospheric convergence and subtropical convergence at 30km. Just a thought. Would the spherical form of the RI make determining this clearer? What about the individual wavenumber diagnostics (see below)? Also, just out of curiosity, why are you not diagnosing the individual wavenumbers as per Eqs. (12) and (13) in Harnik and Lindzen (2001)? I'm certainly okay with using the more traditional 'Matsuno-like' RI and so I am not demanding that you use the individual wavenumber method, rather I am actually just curious for the rationale.

– Answer #6 - We actually used the spherical form of the index of refraction, and had a typo in the caption of Figure 9, which we corrected. Figure 3 below shows the index of refraction (top), meridional (middle) and vertical (bottom) wavenumbers for east, west, and east minus west QBO phases. The differences in the index of refraction are dominated

by the differences in vertical wavenumber. The reviewer is right that there is a stronger meridional wavenumber anomaly in the subtropics (30-40N, 20-30km) during east QBO, however this does not have a very strong signal in the EP flux field on days -10 to -5 (see paper Fig 8). The vertical wavenumber clearly dominates the IR anomalies even in the subtropics, and as indicated by other measures, the increased vertical propagation in east QBO is the main difference. We added a comment on this on page 9 line 24-25.

- Comment #7 –Page 9 lines 19-20: Why exactly is it expected that the nonlinear terms are larger during QBO east? I realize that the QBO east is characterized by more wave driving, but couldn't that appear via the quasi-nonlinear PV flux term (1st term on the RHS of eq. 1) and not via the fully nonlinear terms? I realize that you cite the White et al. (2016) paper in the next sentence, but that just means that your results are consistent. Stating that something is "as expected" seems to imply that there is a physical reason to expect this result.

- Answer #7 - We expected the the nonlinear terms to be larger in the east QBO as we see these events are less reversible. We changed the text to make this point clearer. (page 9 line 17 to page 10 line 2).

- Comment #8 – Page 9 lines 25-28: If I understand your line of reasoning here, you are stating the ZMO3 run has stronger damping in the lower stratosphere and weaker damping in the upper stratosphere. Or said another way, 3d ozone decreases ozone damping in the lower stratosphere but increases damping in the upper stratosphere. You mention in Section 3.1 some of the ozone physics involved, but then you don't mention any of that here. I would say that something interesting can be said regarding what is happening. My initial take would be the following (though for sure the authors should give their own interpretation of the results because I may be missing something). (Note that the discussion below also has implications for your results on page 10 lines 29-35 through page 11 lines 1-9). Based on photochemical and dynamical timescales, the 3d ozone induced decrease in damping in the lower stratosphere must be associated with advection of zonal mean ozone by the wave fields, yes? And in the upper stratosphere, the 3d ozone induced increase in damping is due to photochemistry, yes? Now, the upper stratospheric increase in damping is to be expected based on the ozone-temperature phase relationship dictated by the temperature dependent Chapman chemistry (e.g., Craig and Ohring 1958). However, the lower stratospheric dynamically-based ozone result is fundamentally dependent on the vertical and horizontal ozone gradients. Previous studies have discussed this bit of physics but only in the context of 1D mechanistic models (e.g., Nathan and Cordero 2007 and Albers and Nathan 2012). However, your results are the first to be able to state something more general and thus it may be worth pointing out that it appears that 3d ozone causes dynamically induced ozone heating anomalies that decrease wave damping. This would mean that if there is any seasonal cycle to the vertical and meridional ozone gradients, then there should be some seasonality to the effect of 3d ozone that is perhaps contributing to the enhancement of the HT effect that you describe in your conclusions. Or perhaps the vertical and meridional ozone gradients are different for the wQBO versus eQBO, which in turn leads to some of the differences you see in the EP-flux divergence for the two QBO phases? To be honest, I don't have this all worked out in my head clearly, but it is perhaps worth thinking about because it would seem you might be able to add some physical insight here in the context of a CCM whereas previous studies with physics discussions where limited because of their model simplicity.

I should also mention that you can quite easily see how all of the ozone physics modulate the EP-flux divergence by considering Eq. (14) in combination with Eq. (15) (for the lower stratosphere) and Eq. (17) (for the upper stratosphere) in Nathan and Cordero (2007).

– Answer #8 - The equations for ozone-modified refractive index of Nathan and Cordero (2007) are very insightful for the simplified model, however, in our case, the analysis is complicated by a rich latitude-height structure, and we did not gain a simplified understanding of the role of specific terms.

We distinguish in our answer between a few effects.

1. Zonal mean ozone feedbacks: the effects we discuss in the paper, which amplify the initial radiative perturbation, via a modulation of wave propagation, to a change in the polar vortex and the wave induced overturning circulation, will also change the zonal mean ozone gradients. These changes will feed back onto the initial radiative perturbation we imposed. The sign of this effect, however, is unclear, for the following reason. The ozone induced radiative heating is proportional to the ozone wave amplitude and to the correlation between ozone and temperature waves. The ozone wave 1 amplitude time tendency is dominated by meridional advection (the peaks of ozone wave 1 amplitude follow the peaks in the meridional gradient of the zonal mean ozone (Fig. 4), and the meridional advection term ($v' \frac{d\overline{O3}}{dY}$) is the strongest term in the budget. In the 3DO3 run the meridional gradient is weaker compared to the ZMO3 run. This changes the ozone wave amplitude but not in a straightforward way, because the correlation between ozone and meridional wind also changes, so that the change in ozone wave 1 amplitude has a complex structure with the most significant feature being a weakening at the upper part of the ozone wave peak. This weakening is at the level at which the ozone waves transition from dynamical to radiative control and thus the effect on radiative wave damping is small. At the same time, the lower stratospheric correlation between ozone and temperature wave fields is slightly more positive in the 3DO3 run (Fig. 5), which will result in a weakening of the thermal damping. Thus the sign of the feedback is not clear.

2. A seasonality in the zonal mean ozone and ozone-temperature wave correlation fields: Examining these fields, we find the changes small, consistent with the dominant term in the seasonality of the direct radiative effect being due to the change in zenith angle.

3. A difference in the zonal mean ozone field and ozone-temperature wave correlations between east and west QBO: We repeat the analysis of section 3.2, compositing different fields centered around October upward wave pulses, for east and west QBO phases separately. Fig. 6a shows the life-cycle mean (days -10 to 15) of zonal mean ozone gradients. We see that the largest differences are in the tropical and subtropical region, where the fields are directly forced by the QBO. This causes a weaker ozone wave 1 amplitude in that region during EQBO (Fig 6b). The weaker meridional gradient in the high latitude region also causes a smaller wave amplitude of ozone wave 1 during EQBO

(Fig. 6b), resulting in a weaker ozone direct radiative effect in the lower stratosphere - stronger damping during EQBO events (Fig. 6c). This is also accompanied by a slightly weaker ozone-temperature correlation (Fig. 6d). The temperature wave amplitude, however, is still stronger for east QBO events in the mid-upper stratosphere (Fig. 6e). This suggests the QBO induced changes in the zonal mean ozone field are of secondary order.

These results were partially added on page 6 line 8-9, page 11 lines 16-23.

- Comment #9 – Page 9 Equation (1): Please define your notation here and don't just cite Smith (1983). Specifically, do the different primes mean something different? That is, do the primes in the PV flux term (1st term on the RHS) somehow denote something different from than the primes in the nonlinear terms (2nd and 3rd terms on the RHS)?
- Answer #9 - We took care to define everything carefully and fixed the use of different primes- they were meant to be the same. Besides this we did not find any terms which are not defined.

Minor Comments

- Comment #1 – Introduction lines 1-2: "...exist since the early..." should be "...have existed since the early..."
- Answer #1 - fixed
- Comment #2 – Page 2 line 1: Multi decadal should be hyphenated as multi-decadal.
- Answer #2 - fixed
- Comment #3 – Page 2 line 4: "...(Taylor et al. 2012), does not..." should be "..... (Taylor et al. 2012), do not..."
- Answer #3 - fixed
- Comment #4 – Page 2 line 2: While I could be wrong, I believe that you meant to use the word "assess" and not the word "asses" :)
- Answer #4 - fixed
- Comment #5 – Page 3 line 3: Using a hyphen here doesn't work grammatically. Please rework this sentence.
- Answer #5 - fixed
- Comment #6 – Page 3 line 17: I would suggest also citing the new (ish) paper by Watson and Gray (JAS January 2014) because it provides new insights supporting the original HT-1980 paper, which Garfinkel et al. 2012 (which you cite) call into question.
- Answer #6 - added
- Comment #7 – Page 3 line 21: "noninear" should be "nonlinear".

- Answer #7 - fixed
- Comment #8 – Page 4 line 24: “tendenfcy” should be “tendency”
- Answer #8 - fixed
- Comment #9 – Page 3 lines 24-25: Which figures are you referring to? This is a bit vague.
- Answer #9 - fixed
- Comment #10 – Page 5 line 15: Capitalize “northern hemisphere” (both words)
- Answer #10 - fixed
- Comment #11 – Page 5 line 21: Similar to my Major Comment #4, while the Douglass reference is nice, I really think that the HartmannGarcia 1979 and GarciaHartmann 1980 references are very relevant here and they pre-date the Douglass reference by half a decade. They should also be included.
- Answer #11 -
- Comment #12 – Page 9 lines 3-4: You seem to be stating the same thing twice here (regarding non-acceleration conditions).
- Answer #12 - fixed

Reviewer #2

We thank the reviewer for reading the manuscript and providing their helpful comments. We address their issues below.

- Comment #1 - Much of this paper is based on differences between the top half and bottom half of figure 4. However, the authors don’t appear to have explicitly calculated the statistical significance of the difference between them. The authors need to confirm that the difference between panels 4a and panels 4c, and likewise between panels 4b and 4d, is actually statistically significant.
- Answer #1- To perform this significance test it would be ideal to have many realizations of each simulation (3D or ZM ozone in the radiation code). Since this is not possible with our resources, we do the following:

  1. Take all years of the two simulations - a total of 200 years, and mix them together to one data set of 200 winters.
  2. Randomly choose four groups of winters according to the number of east/west QBO winters for each run (two groups for 3DO3 and two for the ZMO3 run).
  3. Average each group and take the difference between the east and west groups for each simulation.

4. Repeat this 1000 times to get a statistical distribution of 3DO3 minus ZMO3 east minus west QBO anomalies, for each latitude and height grid point.

We now have 1000 differences of random winters for each run. Statistical significance of the 3D(E-W) and ZM(E-W) is calculated by checking if the difference of the E-W (3D-ZM) is bigger/smaller than the 97.5/2.5 percentile of the difference between the two distributions we got.

The result of this calculation is shown in Figure 7 for the zonal mean zonal wind (top) and zonal mean temperature (bot). In the zonal mean zonal winds the negative/positive values in early/late winter indicate that the E-W difference in the 3DO3 run is stronger/weaker than the E-W difference in the ZMO3 run, corresponding to a delay in the HT signal. The differences are statistically significant. The delayed HT signal in the zonal mean temperature is statistically significant as well.

This information was added in the Appendix section.

- Comment #2 - I found figure 12 and its accompanying paragraph to be very confusing. What exactly is Fyy? The y-derivative of the y-component of EP flux? Similar what is Fzz? The z-derivative of the z-component of EP flux? Even if I assume this to be the case, I had serious trouble following the text and the accompanying figure despite multiple rereads. Either the authors need to expand their discussion and help the reader a bit, or remove this entirely as it doesn't appear to be crucial for the rest of the paper.

- Answer #2 - Fyy/Fzz are indeed the y-derivative / z-derivative of the y-component /z-component of EP flux. Following this comment we decided to remove this figure and replaced it with a new one (Figure 12) showing only the EP flux divergence differences between the 3DO3 and ZMO3 runs for east/west QBO events. The relevant text is updated on page 11 line 10-16.

Minor comments:

- Technical comments: The abstract was quite long and wordy. It can almost certainly be shortened without removing key content.

- Answer - the abstract has been re-written.

- Comment #1 - P1, line 8 "in the natural configuration" can be removed. While this may have meaning to someone within the NCAR world, it has little meaning to someone on the outside

- Answer #1 - fixed

- Comment #2 - P2 line 1 chemistry climate models are also used in air pollution studies and for aerosol studies. See the AER-CHEM-MIP project (https://wiki.met.no/aerocom/aerchemmip/start)

- Answer #2 - fixed

- Comment #3 - P2 line 4 the majority . . .. do not
- Answer #3 - fixed
- Comment #4 - P2 line 29 this paragraph extends for 31 lines and is hard to digest! I suggest adding two new paragraph breaks: a first on line 4 of page 3, before “Also”, and a second on line 24 of page 3 before “To understand”
- Answer #4 - fixed
- Comment #5 - P3 line 21 nonlinear is misspelled
- Answer #5 - fixed
- Comment #6 - P4 line 24 tendency is misspelled
- Answer #6 - fixed
- Comment #7 - P4 line 26 I do not understand this sentence. Please rewrite
- Answer #7 - fixed
- Comment #8 - P4 line 28 ozone wave**s**
- Answer #8 - fixed
- Comment #9 - It may be helpful to add an intro sentence to section 3, rather than diving straight into the nitty gritty of the results
- Answer #9 - added
- Comment #10 - P8 line 22 composites is misspelled
- Answer #10 - fixed
- Comment #11 - P9 line 4 sentence is repeated
- Answer #11 - fixed
- Comment #12 - P10 line 34 “descends lower down” it is impossible to infer this from figure 13. This clause should either be removed, or reference made to a different figure.
- Answer #12 - fixed
- Comment #13 - P 11 line 2 the second half of this sentence is very unclear and needs to be rewritten
- Answer #13 - fixed

- Comment #14 - P 11 line 27 I suggest starting a new paragraph with “While”
- Answer #14 - fixed
- Comment #15 - Figure 1 units are not indicated on the colorbar on the left column
- Answer #15 - fixed
- Comment #16 - Figure 5 is missing units
- Answer #16 - fixed
- Comment #17 - Figure 8 is missing the x-label (latitude)
- Answer #17 - fixed (added to last row of the figure, is it enough?)
- Comment #18 - Figure 9 either the caption or the figure itself should state explicitly EQBO-WQBO
- Answer #18 - added to text
- Comment #19 - Figure 13: The caption should note that a thick line indicates statistical significance (assuming I infer correctly).
- Answer #19 - fixed

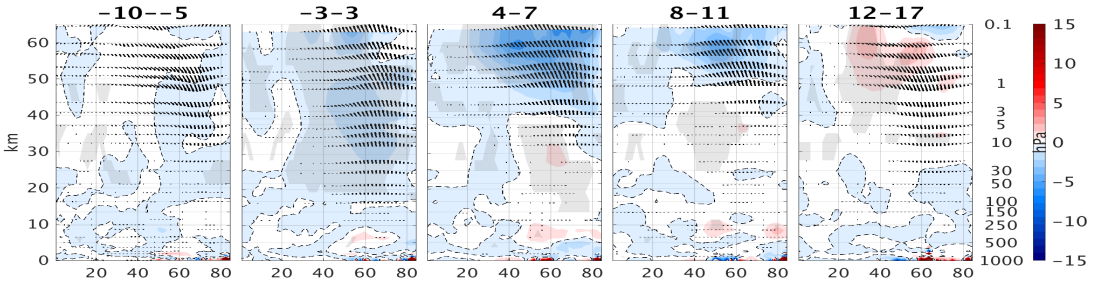

(a) Oct, $\nabla \cdot F$, EQBO ZMO3

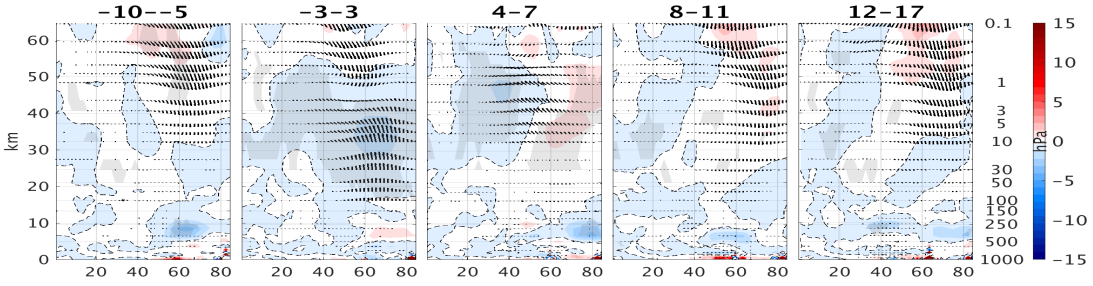

(b) Oct, $\nabla \cdot F$, WQBO ZMO3

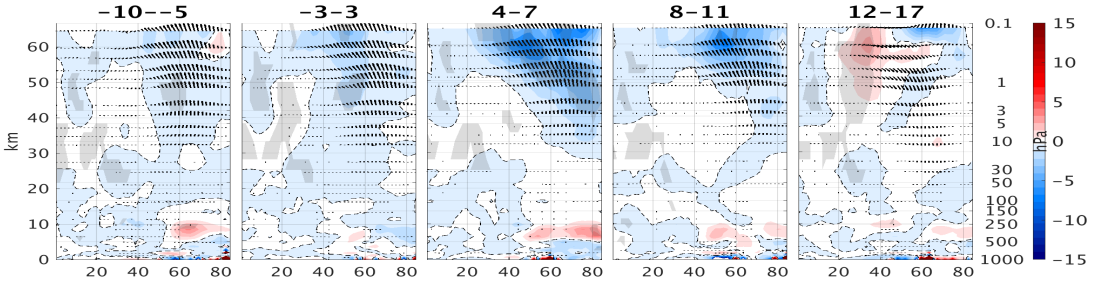

(c) Oct, $\nabla \cdot F$, (E-W)QBO ZMO3

Figure 1. Lat-height time lag composites of EP-flux divergence anomalies from the climatology) for the positive heat flux EQBO (top), WQBO (mid), and the difference between them (bot), for October events (70th percentile of $\overline{V'T'}$ at 50mb 85-45N) of the 3DO3 run. Statistically significant areas are shown by gray shading.

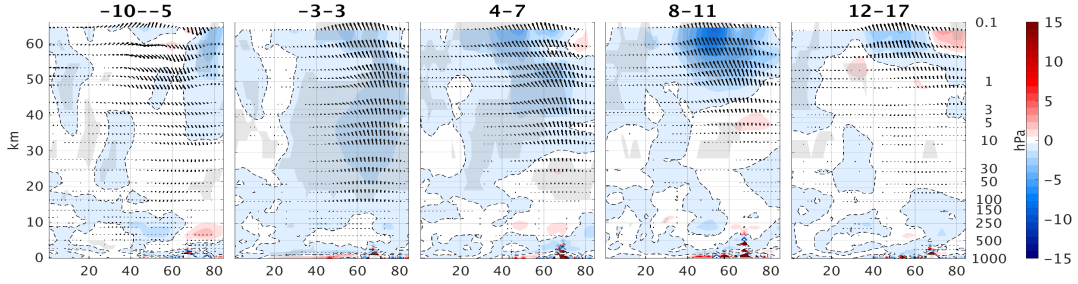

(a) Oct, $\nabla \cdot F$, EQBO ZMO3

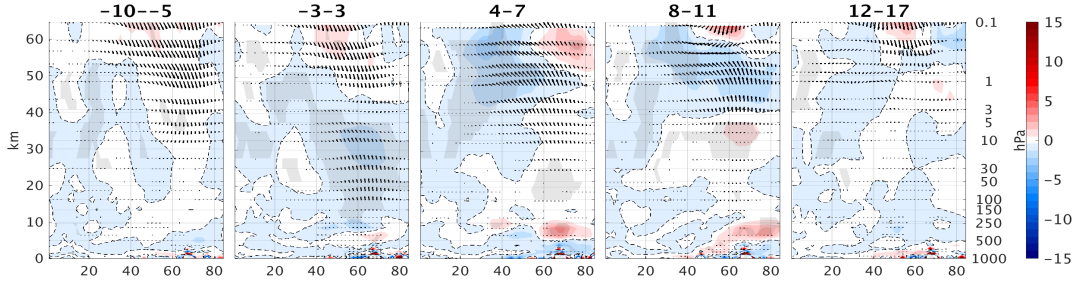

(b) Oct, $\nabla \cdot F$, WQBO ZMO3

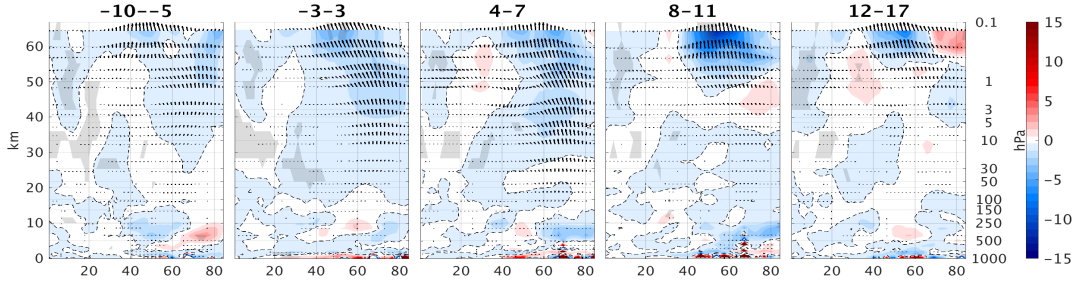

(c) Oct, $\nabla \cdot F$, (E-W)QBO ZMO3

Figure 2. Lat-height time lag composites of EP-flux divergence anomalies from the climatology) for the positive heat flux EQBO (top), WQBO (mid), and the difference between them (bot), for October events (70th percentile of $\overline{V'T'}$ at 50mb 85-45N) of the ZMO3 run. Statistically significant areas are shown by gray shading.

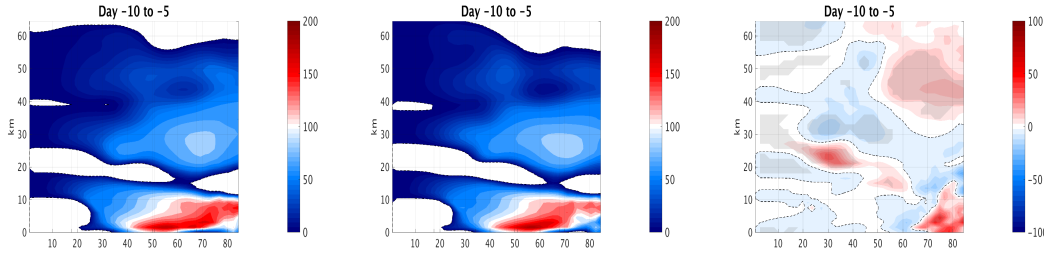

(a) n EQBO (b) n WQBO (c) n E-W

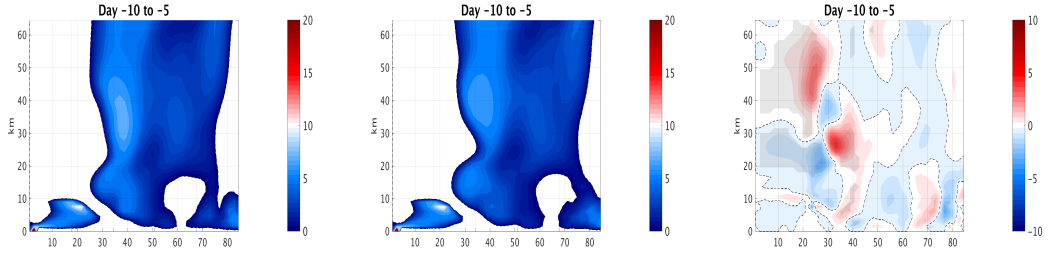

(a) l EQBO (b) l WQBO (c) l E-W

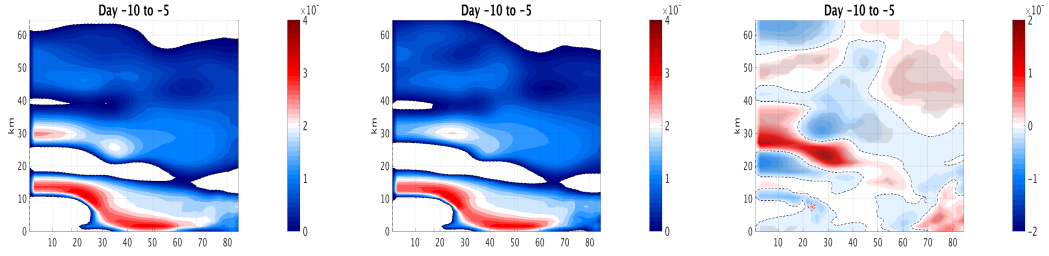

(a) m EQBO (b) m WQBO (c) m E-W

Figure 3. (Top) Index of refraction $\left(n^2 = N^2\left[\frac{a\overline{q}_y}{\overline{U}-c} - \frac{s^2}{cos^2\phi} + a^2f^2F(N^2)\right]\right)$, see eq.C2,5 in Harnik and Lindzen (2001))at days -10 to -5 for east (left), west (center) and the difference between east and west QBO (right) in the 3DO3 run. The meridional and vertical wave components are shown in the middle and bottom row, correspondingly.

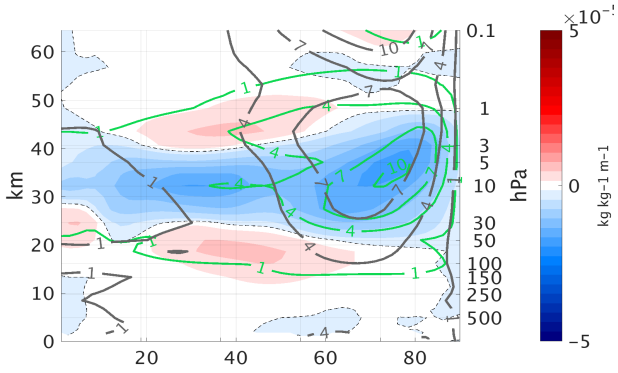

Figure 4. Meridional gradient of the zonal mean ozone (color), ozone wave 1 amplitude (green contours) and temperature wave 1 amplitude (gray contours), for Sep-Nov.

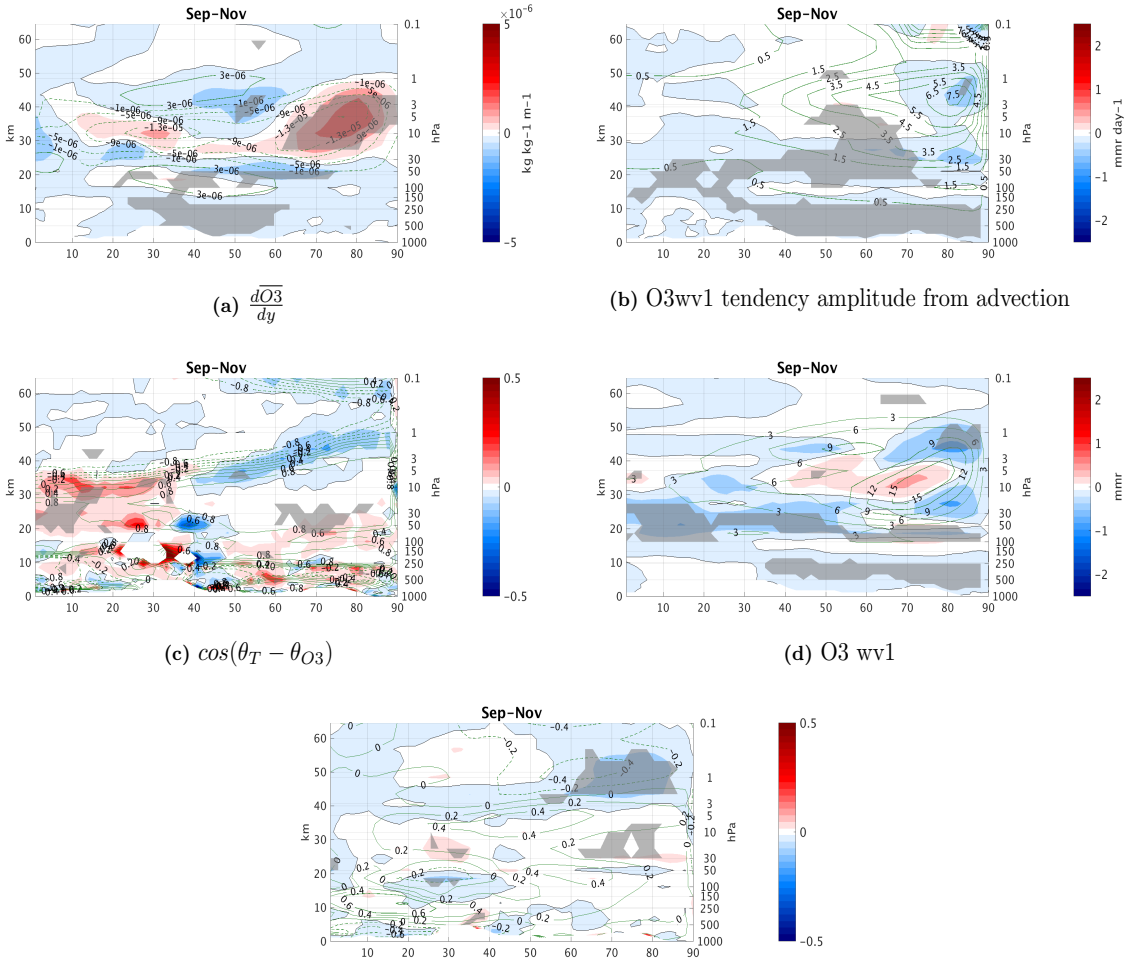

(a) $\frac{d\overline{O3}}{dy}$

(b) O3wv1 tendency amplitude from advection

(c) $cos(\theta_T - \theta_{O3})$

(d) O3 wv1

(e) cos(O3-V) wv1

Figure 5. Latitude-height of 3DO3-ZMO3 (colors) of (a) Meridional gradient of the zonal mean ozone, (b) wave 1 amplitude of the ozone tendency from advection, (c) ozone-temperature correlation for zonal wave 1, (d) ozone wave 1 amplitude and (e) ozone-meridional wind correlation for zonal wave 1, for Sep-Nov. Climatology of the 3DO3 run is shown in green contours.

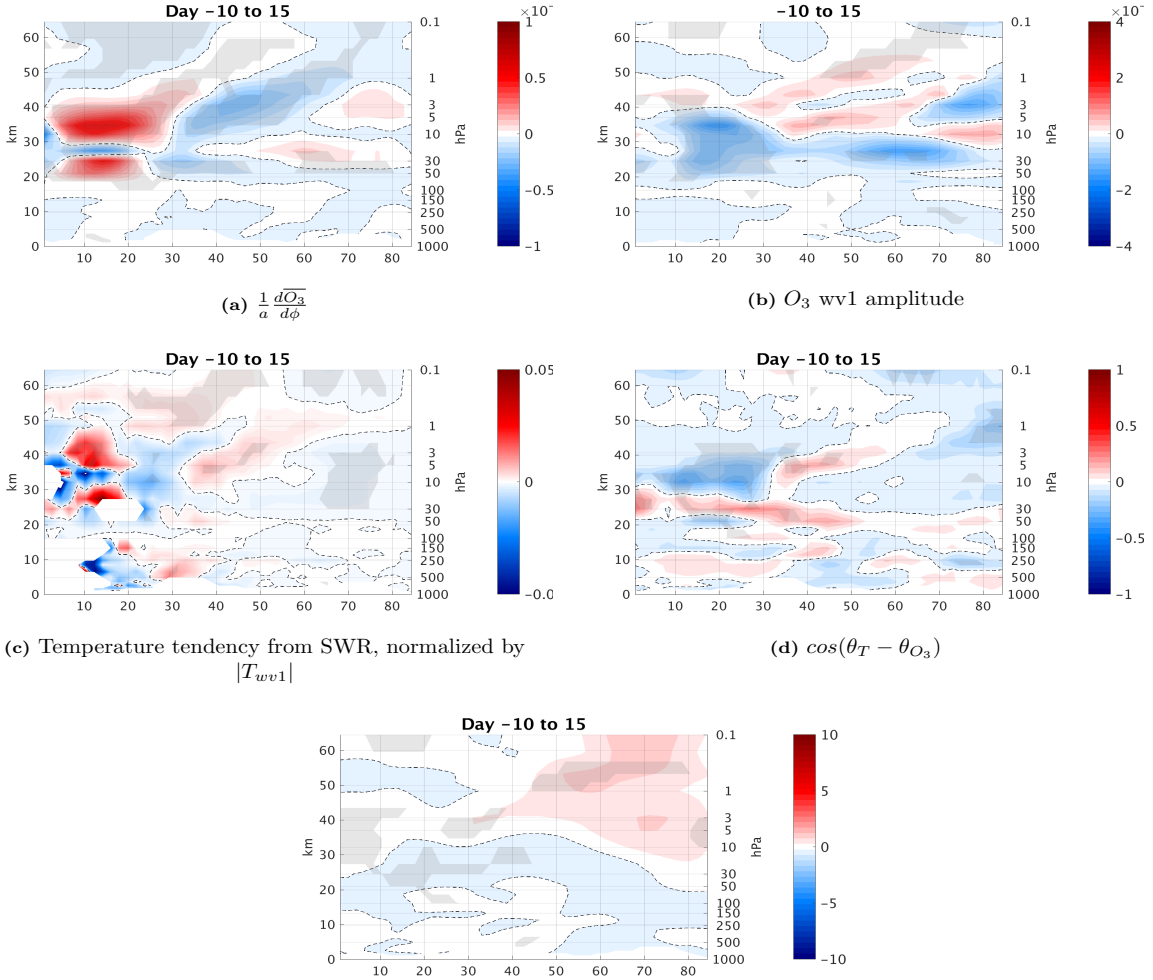

(a) $\frac{1}{a}\frac{d\overline{O_3}}{d\phi}$

(b) O_3 wv1 amplitude

(c) Temperature tendency from SWR, normalized by $|T_{wv1}|$

(d) $cos(\theta_T - \theta_{O_3})$

(e) Temperature wv1 amplitude

Figure 6. Latitude-height of E-W QBO October positive hat flux events composit for day -10 to 15 (a) Meridional gradient of the zonal mean ozone, (b) wave 1 amplitude of the ozone, (c) temperature wave 1 amplitude tendency from short-wave radiation, (d) ozone-temperature correlation for zonal wave 1, and (e) temperature wave 1 amplitude.

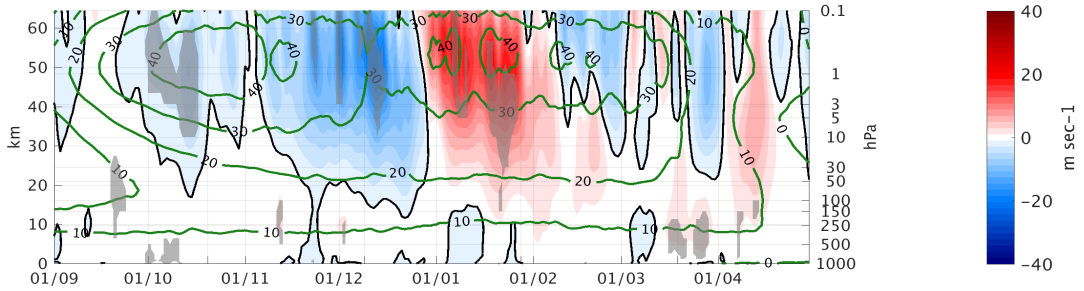

(a) U_{zm}, (E-W)QBO 3DO3-ZMO3

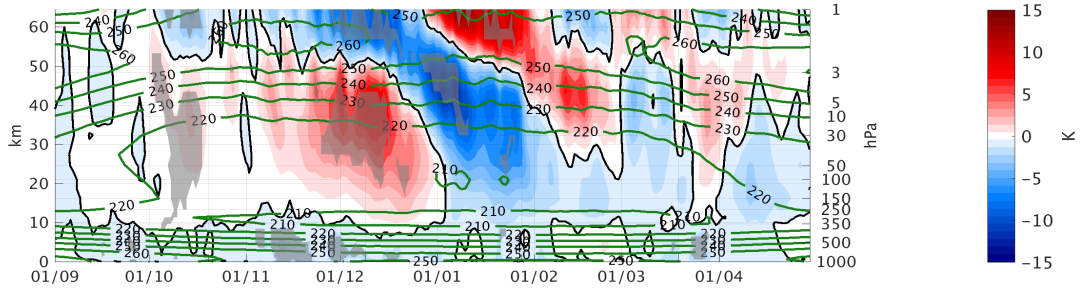

(b) T_{zm}, (E-W)QBO 3DO3-ZMO33

Figure 7. Daily climatology east-west QBO differences between the 3DO3 and ZMO3 model runs of the zonal mean zonal wind averaged over 75-55N (top) and the zonal mean temperature averaged over 90-66N for the 3DO3 (bot), for Sep-Mar. Statistically significant areas are shown by gray shading.

References

Craig, R. A. and Ohring, G.: The temperature dependence of ozone radiational heating rates in the vicinity of the mesopeak, Journal of Meteorology, 15, 59–62, 1958.

Harnik, N. and Lindzen, R. S.: The effect of reflecting surfaces on the vertical structure and variability of stratospheric planetary waves, Journal of the atmospheric sciences, 58, 2872–2894, 2001.

Hartmann, D. and Garcia, R.: A Mechanistic Model of Ozone Transport by Planetary Waves in the Stratosphere, J. Atmos. Sci., 36, 350–364, 1979.

Nathan, T. R. and Cordero, E. C.: An ozone-modified refractive index for vertically propagating planetary waves, Journal of Geophysical Research: Atmospheres, 112, 2007.

Nathan, T. R. and Li, L.: Linear stability of free planetary waves in the presence of radiative–photochemical feedbacks, Journal of the atmospheric sciences, 48, 1837–1855, 1991.

Watson, P. A. and Gray, L. J.: How does the quasi-biennial oscillation affect the stratospheric polar vortex?, Journal of the Atmospheric Sciences, 71, 391–409, 2014.

Radiative effects of ozone waves on the Northern Hemisphere polar vortex and its modulation by the QBO

Vered Silverman[1], Nili Harnik[1], Katja Matthes[2], Sandro W. Lubis[3], and Sebastian Wahl[2]

[1]Department of Geophysical, Atmospheric and Planetary Sciences, Tel Aviv University, Tel Aviv, Israel
[2]GEOMAR Helmholtz Centre for Ocean Research Kiel, Kiel, Germany
[3]Department of the Geophysical Sciences, The University of Chicago, USA

Correspondence to: Vered Silverman (veredsil@post.tau.ac.il)

Abstract.

The radiative effects induced by ~~including interactive ozone, in particular,~~ the zonally asymmetric part of the ozone field ~~,~~ have been shown to significantly change the temperature of the NH winter polar cap, and correspondingly the strength of the polar vortex. ~~However, there is still a debate on whether this effect is important enough for climate simulations to justify the numerical cost of including chemistry calculations in long climate integrations.~~ In this paper we aim to understand the physical processes by which ~~the radiative effects of including interactive ozone , and in particular the radiative effects of zonally asymmetric ozone anomalies (ozone waves), amplify to~~ ozone waves affect can significantly influence the winter polar vortex~~. Using~~ , using the NCAR Whole Atmosphere Community Climate Model~~in the natural configuration, in which~~ , run with 1960s ozone depleting substances and green house gases~~are fixed at 1960's levels, we~~ . We find a significant effect on the winter polar vortex only when examining the QBO phases separately~~. Specifically, the seasonal evolution of the midlatitude signal of the QBO - the Holton–Tan effect -~~ , since the ozone waves affect the vortex in an opposite manner during the different QBO phases. Moreover, the emergence of a midlatitude QBO signal is delayed by one to two months when radiative ozone wave effects are removed. ~~Since the ozone waves affect the vortex in an opposite manner during the different QBO phases, when we examine the full time series, besides~~ The influence of ozone waves on the winter polar vortex, via their modulation of short wave heating is not obvious, given that short wave heating is largest during fall, when planetary stratospheric waves are weakest. By combining an analysis of wave 1 amplitudes of temperature perturbations using explicit temperature time tendency terms, along side a synoptic analysis of upward planetary wave pulses, we are able to show the chain of events that leads from an early fall direct radiative effect ~~, we find no statistically significant winter effect. We start by quantifying the direct radiative effect of ozone waves on temperature waves, and consequently on the zonal mean zonal wind, and show that this effect is most significant during early fall. We then show how the direct radiative effect amplifies by modifying the evolution of individual upward planetary wave pulses and their induced mean flow deceleration during early winter when stratospheric westerlies just form and waves start propagating up to the stratosphere. The resulting mean-flow differences~~ on the upward propagating planetary waves when they are still very weak, to a winter polar vortex modulation. We show that an important stage of this amplification is the modulation of individual wave life cycles, which accumulate during fall and early winter, ~~after which they get amplified through~~ before being amplified by wave-mean flow feedbacks. We find that the evolution of these

early-winter upward planetary wave pulses and their induced stratospheric zonal mean flow deceleration ~~are~~ is qualitatively different between QBO phases, providing a new mechanistic view of the extratropical QBO signal~~(the Holton-Tan effect)~~. We further show how these differences result in an opposite ~~effect of the~~ radiative ozone wave ~~perturbations on the mean flow deceleration for~~ effect between east and west QBO~~phases~~.

1 Introduction

Chemistry climate models (CCMs), which calculate ozone interactively and therefore include asymmetric ozone effects, ~~exist~~ have existed since the early 2000s (CCMVal, 2010). Due to their large numerical cost, CCMs have mostly been used ~~for stratospheric processesonly~~ to study stratospheric processes, and only in recent years they have been coupled to an interactive ocean for the purpose of performing ~~multi-decadal climate simulations~~multi-decadal climate simulations, air pollution, and aerosol studies. There is still an ongoing debate whether interactive atmospheric chemistry, which is computationally very expensive to run for long-term climate integrations, is required in order to generate an appropriate climate signal. The majority of the fifth Coupled Model Inter-comparison Project (CMIP5) models (Taylor et al., 2012) ~~does~~ do not use interactive atmospheric chemistry, instead they prescribe a zonal mean monthly mean ozone field, thus neglecting the effects of zonal asymmetries in the ozone field (ozone waves). In the upcoming CMIP6 exercise (Eyring et al., 2016) more climate models will perform simulations which will include atmospheric chemistry, however, a majority will still use prescribed ozone fields. One of the main processes missing from simulations with prescribed ozone fields is the formation and interaction of ozone zonal asymmetries (ozone waves). In order to compare and evaluate the performance of models using either interactive chemistry (including ozone waves) or prescribed zonal mean ozone (neglecting ozone waves), it is crucial to understand the impact of ozone waves on stratospheric dynamics.

~~The effects of ozone waves can be formulated as an effective change in the temperature-wave Newtonian damping rate (the rate at which temperature perturbations are relaxed towards the mean state from which they deviate (Hartmann, 1981)). Whether the damping is enhanced or reduced depends on the spatial correlation of ozone and temperature perturbations. For example, when both ozone and temperature perturbations are positive, there is an increase in shortwave ozone heating due to its higher concentration, effectively reducing the damping of the temperature perturbation.~~

Albers and Nathan (2012) suggested two pathways through which ozone waves can affect the stratosphere. First, by affecting ozone advection through wave-ozone flux convergence, the zonal mean heating rate changes, consequently affecting the zonal mean temperature and wind. Second, the radiative effect of ozone waves impacts the temperature waves, and correspondingly the damping and propagation properties of planetary waves, and their ~~EP-flux~~EP flux. Albers and Nathan (2012) further showed that the latter radiative effect reduces the planetary wave drag and modifies the wave amplitudes in a 1-dimensional Holton-Mass model (Holton and Mass, 1976) coupled to a simplified ozone equation. These result in a colder upper stratosphere and a stronger polar vortex. In our paper we will focus on the second pathway - the direct radiative effect of ozone waves.

The radiative effects of ozone waves can be formulated as an effective change in the Newtonian damping rate of temperature waves (the rate at which temperature waves are relaxed towards the mean state from which they deviate (Hartmann, 1981)).

This stems from the correlations between ozone and temperature perturbations. A correlation between ozone and temperature is expected both because temperature directly affects ozone destruction processes, and because advection is a main contributor to both ozone and temperature anomalies (Douglass et al., 1985b). Depending on the sign of the spatial correlation of ozone and temperature perturbations, the Newtonian damping rate can be enhanced or weakened. For example, when both ozone and temperature perturbations are positive, there is an increase in shortwave ozone heating due to its higher concentration, effectively reducing the damping of the temperature perturbation.

Several approaches have been used to ~~asses~~ assess the effect of ozone waves in GCMs. Some studies included the climatological ozone waves~~in a~~ , either constant or seasonally varying~~specified ozone field (Gabriel et al., 2007; Crook et al., 2008; Peters et al., 2015) . While these~~ , in their specified ozone fields (Gabriel et al., 2007; Crook et al., 2008; Peters et al., 2015). These studies found a significant effect ~~for~~ of including ozone waves, however they do not include ~~the dynamical interaction~~ any interactions between the ozone waves and ~~other~~ the wind and temperature wave fields. A more direct approach ~~is comparing two model simulations, one which includes ozone waves in the radiative transfer code and the other with~~ to assessing the radiative effect of ozone waves has been to compare a full model simulation with one in which ozone is fully interactive but only the zonally symmetric part of the ozone field is passed onto the ~~radiation code. These~~ radiative transfer calculation. Such studies found that ~~the runs which include ozone waves had a weaker~~ , including the radiative effects of ozone waves resulted in a weaker and warmer northern winter polar vortex (Gillett et al., 2009; McCormack et al., 2009), stronger planetary wave drag, and a higher frequency of sudden stratospheric warmings (McCormack et al., 2009; Albers et al., 2013; Peters et al., 2015)~~. However, there were some discrepancies regarding~~ , though the timing and strength of these effects were different between the studies. For example, McCormack et al. (2009) found the weakening of the polar vortex to occur in mid-Jan-Feb, while Gillett et al. (2009) found the weakening to occur earlier in Nov-Dec. We will discuss a possible explanation for this in the Summary.

~~A puzzling aspect of these results is the following. The radiative effects of ozone anomalies are~~ Considering the seasonal evolution and spatial structure of solar radiative forcing and stratospheric waves, the above radiative effect of ozone waves on the mid-winter polar vortex is not obvious. While solar radiative forcing is expected to be strongest in summer and at lower latitudes, ~~where solar radiation is strongest, while planetary waves , and in particular ozone and temperature waves, are largest~~ the planetary waves on which this forcing acts are strongest in winter and at high latitudes. ~~Thus it is not clear how the~~ It is clear that the significant change in the mid-winter polar vortex stems from an amplification of the direct radiative influence of ozone waves~~affects the mid winter vortex – whether it is a seasonal amplification of an early fall radiative effect~~, however it is not clear if it is an amplification of a weak early-fall radiative modification of the weak fall waves, or whether ~~it is a mid-latitude amplification of radiative changes at the subtropical edge of the waves. For this~~ a radiative effect on the subtropical flank of the stronger midwinter waves is what gets amplified. To answer this question, we first need to ~~determine the radiative effect~~ quantify the radiative influence of ozone waves on the ~~wave temperature - to quantify the influence on thermal damping of temperature waves~~overall thermal wave damping, and then to examine how this direct radiative effect gets amplified via wave-mean flow interactions to modify the polar vortex. This has not been explicitly examined using a CCM before. ~~Also, given the possible involvement of~~

In other contexts of a solar influence on the polar vortex, like the 11-year and 27-day solar cycles, the ~~subtropics, we need to examine the influence of the~~ solar effect is strongly dependent on the phase of the Quasi-Biennial ~~Oscillation (QBO) - a tropical phenomenon in which the zonal mean zonal wind alternates from easterlies to westerlies, while the signal descends from the upper stratosphere with a mean period of approximately 28 months. An effect of the tropical flow on mid-latitudes is known to exist for the QBO, the phase of which is defined based on the direction of winds in the lower stratosphere. Interestingly, the QBO plays a role in communicating the effects of solar variations to high latitudes. Numerous studies have shown that the 11-year solar cycle correlates with the Arctic polar vortex (~~Oscillation (QBO, e.g. ~~, Labitzke and Van Loon (1988); Labitzke et al. (2006); M~~ ~~). However, this signal correlates differently depending on the~~ Labitzke and Van Loon (1988); Labitzke et al. (2006); Matthes et al. (2010);). For example, during the westerly phase of the QBO~~: in the westerly phase~~ , solar maximum conditions correlate with a weak and warm polar vortex, while ~~in the easterly QBO phasesolar max~~ during the easterly phase, solar maximum conditions correlate with a stronger polar vortex. ~~These studies suggest that the influence of radiative effects on the atmospheric circulation might depend on the phase of the QBO~~Another way to view this connection is that the solar forcing modulates the midlatitude effect of the QBO (a stronger wave deceleration of the polar vortex during east QBO), with the midlatitude QBO signal being different during solar maximum and solar minimum. It is thus also plausible that the ~~QBO modulates the effects~~ radiative effect of ozone waves ~~at polar latitudes during winter as well.~~ on the polar vortex depends on the phase of the QBO, and can be understood as a modulation of the midlatitude QBO signal.

The QBO affects the propagation of waves in the stratosphere, resulting in a weaker and warmer winter polar vortex in the ~~northern hemisphere during QBO east~~ Northern Hemisphere during east QBO conditions (the Holton-Tan effect) (Holton and Tan, 1980). Several studies ~~suggested a mechanism~~ have suggested mechanisms to explain this relationship. ~~For example,~~ Holton and Tan (1980) suggested that the poleward position of the subtropical zero wind line focuses the planetary wave activity to the polar vortex region during ~~QBO east conditions, while~~ east QBO conditions. This was recently supported by Watson and Gray (2014), who analyzed the short-term transient response to imposed nudging towards easterly QBO tropical winds. On the other hand, Ruzmaikin et al. (2005) and Garfinkel et al. (2012) found that the subtropical meridional circulation of the QBO in the upper stratosphere is responsible for increased ~~EP-flux~~ EP flux convergence in the polar vortex region. ~~White et al. (2016) suggested the early winter planetary waves propagate differently and are more nonlinear under west QBO conditions.~~ Gray et al. (2001) found that not only ~~winds in the tropical lower stratosphere but also in the upper stratosphere~~ lower stratospheric tropical winds (which define the QBO phase), but also upper stratospheric tropical winds, influence the polar night jet. The Holton-Tan effect in observations is found to be ~~more robust~~ robust starting in early winter ~~(Holton and Tan, 1980), and we will see how this can be important to understand the influence of ozone planetary waves on the seasonal development of~~ (Holton and Tan, 1980; Watson and Gray, 2014), though in some models it appears only later in the season (e.g. Watson and Gray (2014)). The late winter QBO signal is generally attributed to a modulation of the ~~winter polar vortex. To understand the mechanism through which ozone waves affect the high latitude QBO signal~~ formation of sudden stratospheric warmings (Anstey and Shepherd, 2014), while the early winter signal has not been discussed so much. Recently, White et al. (2016) suggested that the early winter planetary waves propagate differently and are more nonlinear under east QBO conditions.

In this paper we will concentrate on the early winter midlatitude QBO signal and its modification by the radiative effect of ozone waves. To do this, we will take a synoptic approach, and analyze the life cycles of individual upward propagating wave events during fall, when the westerlies just get established in the stratosphere and planetary waves start propagating up from the troposphere. Besides illuminating the role or radiative ozone wave effects, this approach also provides a new look at how the tropical winds affect the polar vortex and the seasonal development of winter.

We will start by describing our model setup and output terms (Sec. 2). We will then show and quantify the direct radiative ozone wave effects in terms of a modulation of the radiative damping (Sec. 3.1), and their corresponding influence on the atmospheric circulation (Sec 3.2). Section 3.3 will discuss the modulation of the seasonal cycle of the QBO and the Holton-Tan effect. Conclusions will be discussed in the last section. Radiative ozone wave effects during summer are discussed in the appendix.

2 Methodology

2.1 The WACCM Model

The model simulations were run with NCAR's CESM version 1.0.2, consisting of atmosphere (WACCM), ocean (POP), land (CLM), and sea ice (CICE) components, based on the Community Climate System Model (CCSM4; Gent et al. (2011)). The atmospheric component used for our experiments is the Whole Atmosphere Community Climate Model (WACCM) version 4 (Marsh et al., 2013) which has a horizontal resolution of 1.9°x 2.5° (latitude,longitude), 66 levels up to about 140 km, and interactive chemistry (MOZART version 3). The chemistry module includes a total of 59 species, such as Ox, NOx, HOx, ClOx, BrOx, and CH4, and 217 gas phase chemical reactions (Marsh et al., 2013). The model has a nudged Quasi-Biennial Oscillation (QBO). The nudging is done by relaxation of the tropical zonal winds between 22S-22N, from 86 to 4 hPa towards an averaged QBO cycle including a relaxation zone to the north and south. The QBO nudging is based on two idealized ~~QBO-east and QBO-west~~ east-QBO and west-QBO phases based on observational (rocketsonde) data, see further details in Matthes et al. (2010). Having a QBO in the model is important for a realistic representation of the interaction between the tropical and extra-tropical region. The solar cycle is prescribed as spectrally resolved daily variations following (Lean et al., 2005).

In our model experiments we kept greenhouse gases (GHGs) and ozone depleting substances (ODSs) fixed at 1960's concentration levels (pre ozone-hole) to get the cleanest signal possible for the ozone wave effects. Each experiment is a freely running 100-year simulation (1955-2054) with interactive ocean and sea ice components. We run two 100-year simulations, one using the full ozone field when calculating the radiative heating rates (hereafter 3DO3 run), and one using the zonally averaged ozone field in the radiation code (hereafter ZMO3 run, see Table 1). To clarify, we use the ozone field in the advection scheme, keeping the effect of ozone waves through the first pathway suggested by Albers and Nathan (2012), as we are interested only in the direct radiative effect of ozone waves. In the ZMO3 run we use the full, zonally varying, ozone field above 1hPa in the radiation code to avoid anomalous heating in the lower mesosphere due to the daily cycle (Gillett et al., 2009). We transition from zonally averaged ozone to a full ozone field between 2hPa to 1hPa.

2.2 Diagnostics

~~We explicitly output the~~ To evaluate the different terms in the wave temperature budget, we explicitly output temperature time tendency terms from shortwave and longwave radiation, ~~as well as from dynamics~~dynamics, and non-conservative processes. We use ~~the explicit time tendency~~ these terms to evaluate the direct ~~effect of ozone waves on the temperature wave damping, and to~~ ozone-wave radiative effect, and compare it to other temperature time ~~tendenfcy~~ tendency terms, in particular dynamics (see Figures for details).

The radiative effects of ozone modulate the planetary waves, and ~~so does their influence of~~ correspondingly their influence on the mean flow. These differences add up to a difference in the climatological mean. We find that the effects of ozone waves are QBO dependent. To understand the differences in planetary wave propagation depending on the phase of the QBO, and how ozone ~~wave~~ waves modulate them, we look at the life cycles of individual events of upward wave propagation from the troposphere to the stratosphere. ~~To do this, first we calculate the daily $\overline{V'T'}$ at 85-45N,~~ The upward wave events are chosen based on the daily 100hPa ~~, for both ZMO3 and 3DO3 runs. We then find, for each month, the 70th percentile of the heat flux time series of both runs and select all the~~ meridional heat flux ($\overline{V'T'}$), averaged between 45-85N. We chose the 100hPa level since this is the region where the waves enter the stratosphere, however, repeating the analysis for events chosen using the 50hPa level did not qualitatively change our results. We choose all days for which ~~the $\overline{V'T'}$ value exceeds this~~ this heat flux index exceeds the 70th percentile~~threshold~~, calculated for each calendar month from both ZMO3 and 3DO3 runs. We sort consecutive days into a single event, and events which are separated by less than 5 days are considered as a single events. The central day of the event is considered as the day of the highest ~~$\overline{V'T'}$ value. Then we~~ $\overline{V'T'}$ value. We classify the events for east/west QBO according to the phase of the QBO~~using the monthly zonal mean zonal wind during the same month~~. The number of events for each month and model configuration is listed in Table 2. Similar results were found for higher ~~$\overline{V'T'}$~~ $\overline{V'T'}$ thresholds, but the number of events was smaller. We will mostly examine the upward wave events ~~in fall , during which there are~~ during the fall season, which has no negative heat flux ~~(~~events (no downward wave coupling)~~events~~. The phase of the QBO is chosen using the zonal mean zonal wind at $50-30hPa$, between $2.8S-2.8N$ around the equator (u_{QBO}), where easterly ~~(westerly)~~ and westerly QBO winters are chosen ~~where $u<-2.5\frac{m}{sec}$ ($u>5\frac{m}{sec}$) during December.~~ when $u_{QBO}<-2.5\frac{m}{sec}$ and $u_{QBO}>5\frac{m}{sec}$ respectively, based on the value of winds during October each winter (choosing December made no difference) The statistical significance of the differences between two model runs (e.g. east - west QBO or 3DO3 - ZMO3) is computed using a two-tailed t-test, with differences exceeding the 5% significance level marked by gray shading.

3 Results

In this section, we start with evaluating the influence of the direct radiative effect on temperature wave damping, and consequently on the wave-mean flow interaction, during autumn. We then examine the implication of these effects on the seasonal cycle of the autumn-winter season, by inspecting the differences between our two simulations, with and without ozone waves passed

onto the radiation code. We will see how the influence of ozone wave effects depends on the propagation of planetary waves in the vertical and meridional directions, and how this depends on the phase of the QBO.

3.1 The Direct Radiative Effect

~~Radiative effects of ozone waves~~ Ozone waves, via their influence on short wave radiative heating, modulate the radiative damping ~~rate~~ of temperature waves (see Appendix) in a way which depends on the spatial correlation between ozone and temperature waves (Craig and Ohring, 1958). In the photochemically controlled upper stratosphere (above 10hPa) this correlation is negative, and in the ~~transport controlled~~ transport-controlled lower stratosphere (below 10hPa) the correlation is generally positive (Douglass et al., 1985a; Hartmann, 1981). The negative correlation in the photochemically controlled region follows naturally from the temperature dependence of ozone destruction (Craig and Ohring, 1958). The positive correlation in the dynamically controlled region is not as obvious, since it depends on the correlation between the ozone, and the merdional and vertical winds wave perturbations, as well as on the vertical and meridional gradients of zonal mean ozone (e.g. Hartmann and Garcia (1979)). In our simulations, meridional advection of ozone is the dominant term, and correspondingly ozone wave 1 amplitudes peak where the meridional gradients of the zonal mean ozone are strongest (not shown).

The short-wave time tendencies of zonal wave 1 temperature amplitude ~~is~~ are shown in Figure 1, alongside the wave 1 temperature and ozone amplitudes for reference, for ~~northern hemisphere~~ Northern Hemisphere summer (Jun-Aug), fall (Sep-Nov), and winter (Dec-Feb). The tendencies were calculated using equation A2. The magnitude of the short-wave time tendency varies from $\pm 0.1 \frac{K}{day}$ to $\pm 0.2 \frac{K}{day}$, while the total tendency is about $\pm 0.5 \frac{K}{day}$ (not shown). It is generally positive in the lower stratosphere and negative in the upper stratosphere, with the zero line shifting from 5hPa in the tropical region to 2-3hPa at higher latitudes (Fig. 1a,1c,1e). The positive ~~correlation~~ time tendency at lower levels is due to the spatial correlation of ozone and temperature being positive in this region (not shown), as a result of ozone being dynamically controlled there (Douglass et al., 1985b). The negative tendency at upper levels is due to the negative correlation between ozone and temperature due to ozone being chemically controlled at high altitudes (Douglass et al., 1985b). As predicted by previous theoretical studies, we find that ozone wave radiative effects decrease (increase) the temperature wave damping where this correlation is positive (negative). This is also in agreement with Nathan and Cordero (2007) who found similar ozone wave effects in a coupled-ozone chemistry Holton-Mass model. This is true for zonal waves 2-4 as well (not shown). During summer, although the wave amplitudes are small (around 1K), the radiative effects coincide with the peak of the waves (Fig. 1b). This is also the case during fall, when the radiative effects are significant in the region where the temperature and ozone waves peak (around $7K$ and $7 \cdot 10^{-7} \frac{kg}{kg}$ respectively, $60-80N$, $10-1hPa$). To get a sense of the importance of the short-wave effect on temperature wave amplitudes, we explicitly calculate the ratio between this term and the corresponding time tendency due to long wave radiation (the radiative damping term, Figure 1, right column). We find that the shortwave ~~tendency can reach up to~~ time tendency reaches 40% of the longwave time tendency (Fig. 1d)~~, however~~ . Later in winter, when the waves are stronger ~~later in winter~~ (around $16K$ and $10 \cdot 10^{-7} \frac{kg}{kg}$, $50-80N$, $10-1hPa$), the radiative effects ~~at the region of peak wave amplitude are small (up to~~ are weak at the peak of the temperature waves (around 10%, Figure 1f)~~as a result of radiation being weaker~~ , because the radiation is weak at higher latitudes~~during this period~~. These results are consistent with Nathan and Li (1991)

who showed that ozone wave effects are strongest during September, and weakest during January due to the large solar zenith angle.

We further quantify ~~total wave-amplitude weighted temperature time tendencies~~the total wave-weighted time-tendency ratio, for each calendar month separately, as follows:

$$\int_{month} \frac{\int f(|T|) \cdot |T| dydz}{\int |T| dydz} dt$$

where $f(|T|) = \frac{d|T|_{tend1}}{d|T|_{tend2}}$, ~~and~~ with the subscripts tend1 and tend2 ~~are different daily temperature~~ denoting two different time tendency terms, calculated from daily wave 1 ~~amplitude time tendency terms~~temperature amplitude time tendencies, averaged over 80-50N, 70-3mb. The ratios ~~of~~ between the different time tendency terms ~~for each of the months Sep-Dec~~ are shown in Table 3. We find that the relative shortwave contribution (columns 1-2) is strongest ~~in~~ during fall (Sep-Oct) when there is enough radiation and the waves start to increase (about 19% of the longwave cooling and 8% of the dynamical time tendency terms during October). By November~~this~~, the relative shortwave contribution decreases by 50%, while the total radiative contribution increases compared to dynamics (3rd column) due to a stronger decay of the wave through longwave radiation (4th column). We thus expect the direct ozone wave effect to have the strongest influence during Sep-Oct. In December, the dynamics play a larger relative role, indicating the waves are becoming more non-linear. We will show in Section 3.4 how these radiative effects ~~in fall influence the differences in east/west QBO and~~ during fall modify the QBO signal at high latitudes and the mid winter polar vortex.

3.2 Radiative ozone wave effects on the atmospheric circulation

In this section we examine the differences in the circulation between the model run with full ozone fields passed to the radiation code (3DO3), and the run with the zonal mean ozone ~~used for stratospheric heating rate calculations~~ passed onto the radiation code (ZMO3), as described ~~is~~ in Section 2.1. The short-wave radiative forcing of temperature waves in the 3DO3 model run (~~Shown~~ shown for wave 1 in Figure 1) constitutes the primary difference in wave forcing between the two runs. Thus we expect the 3DO3 run to have weaker temperature wave damping in the lower to mid stratosphere, and stronger wave damping in the upper stratosphere.

The differences in the seasonal cycle of the polar cap temperature and the polar vortex strength (the zonal mean zonal wind ~~at mid-high latitudes (~~averaged over $55 - 75N$), between the 3DO3 and the ZMO3 runs are shown in Figure 2 (gray shading shows regions of statistical significance at 5% significance level). We see a significant effect ~~in~~ during fall, when both the waves and radiation are strong enough (Section 3.1) and the vortex is established (green contours in Figure 2b). The polar night jet is stronger in the lower stratosphere and weaker in the upper stratosphere in the 3DO3 run, with the upper stratospheric effect lasting until November (Fig. 2b). This is consistent with a weaker wave damping and thus stronger waves in the lower stratosphere, and stronger wave damping and thus weaker waves in the upper stratosphere (Fig. 1c). Correspondingly, the westerly jet is stronger in the lower stratosphere ~~is stronger,~~ and weaker in the upper stratosphere, as a result of an upward shift of the ~~wave absorption~~ wave-absorption region (see next paragraph).

The above results suggest that the radiative effects of ozone waves ~~in the 3DO3 run are most robustly established~~ are most robust during Sep-Oct, (Fig. 2), when the winter vortex ~~establishes~~begins to be established, solar radiation reaches high latitudes, and the waves are strong enough to be radiatively affected, ~~and~~ while still weak enough for dynamics not to dominate completely. Under these conditions, the direct thermal damping of temperature waves by ozone waves has the largest influence. To understand how the ozone effects translate to dynamical changes, we examine the latitude-height structure of zonal wave 1 temperature and its shortwave radiative time tendency, the zonal mean zonal wind~~and EP-Flux~~, and the EP flux convergence, during September (Fig. 3). We find that the temperature wave 1 amplitude is stronger throughout the stratosphere due to the weaker damping in the lower stratosphere (Fig. 3b), resulting in an upward displacement of the ~~EP-flux~~ EP flux convergence region where the waves decelerate the mean flow (Fig. 3c). Explicitly, there is decreased ~~EP-flux~~ EP flux convergence in the polar stratosphere, where the wave damping is reduced (note the ~~gray lane marking the zero~~ grey line marking where the short wave radiative damping ~~line~~changes sign), and increased ~~EP-flux~~ EP flux convergence in the upper stratosphere/lower mesosphere where the wave damping is stronger~~, and~~. The EP flux convergence also increases at lower latitudes, where more wave activity reaches due to the reduced high latitude convergence (Fig. 3a). This causes the polar night jet to strengthen in the lower stratosphere and weaken in the upper stratosphere, with a poleward tilt (Fig. 3d), ~~while the latter lasts~~ with the upper stratospheric deceleration lasting until November (Fig. 3d). The ~~robust direct effects during September disappear~~ above robust direct radiative effect disappears after November (Fig. 2)~~. This is most likely the~~, most likely as a result of the ~~weak shortwave radiation at high latitudes and the dynamical effect taking over.~~ seasonal reduction in shortwave radiation and the strengthening of the dynamical processes. Nathan and Li (1991) found that when the waves peak in the region where ozone and temperature are positively correlated, the main ozone-wave effect is to strengthen the waves due to the weaker radiative damping, whereas when the waves peak higher in the region of negative ozone-temperature correlation, the dominant ozone-wave effect is the increased radiative damping. In our model we see the dominant effect is to increase wave amplitudes throughout the mid-latitude stratosphere. Apart from the obvious model differences (1D vs CCM) it is possible this is also due to the fact that in the ZMO3 run, we zonally average the ozone field only in the stratosphere, in order to avoid large biases from tides in the mesosphere.

The results shown in Figure 2 appear to suggest that the winter mid latitude stratosphere is not sensitive to the inclusion of radiative ozone wave effects. While there is a significant radiative effect during fall, it seems to disappear later on. In the next section we will show, however, that this lack of a response is due to the response being oppositely signed between east and west QBO phases, so that there is a cancellation when all years are considered. ~~A dependence of the mid-latitude response to various forcings on the phase of the QBO has been observed before in context of solar forcing, both for the 11-year solar cycle (Labitzke and Van Loon, 1992) and for the 27-day period (Garfinkel et al., 2015). In the next section we will thus examine the response of the midlatitude QBO signal to the inclusion of ozone waves in the radiation code.~~

3.3 The ~~modulation~~ onset of the midlatitude QBO signal in fall and its modulation by ozone waves

The influence of the tropical QBO phenomenon on the extra-tropical region~~results in~~, known as the Holton-Tan effect, consists of a weaker and warmer polar night vortex during the easterly phase of the QBO~~, known as the Holton-Tan effect~~. Figure 4

shows the ~~difference between the east and west QBO phases of the seasonal evolution of the polar vortex~~ east minus west QBO seasonally varying polar vortex strength and polar cap temperatures, ~~overlain on~~ alongside the climatological seasonal cycle based on all years, for the 3DO3 and ZMO3 runs. In the 3DO3 run, the Holton-Tan effect starts in October, ~~where the vortex is weaker~~ with a weaker vortex (Fig. 4a) and ~~warmer~~ a warmer polar cap (Fig.4b) ~~in~~ during the easterly QBO phase. In the ZMO3 run (Fig. 4c-4d), the Holton-Tan effect is delayed, with the robust signal starting about two months later, in January instead of November. The calculation of the statistical significance for the difference between the top panel and the bottom panel of Figure 4 is described in Appendix A1.

In order to understand the different seasonal development of the ~~polar vortex, we will first examine the differences between east and west QBO in the~~ midlatitude QBO signal between 3DO3 ~~run when they just start, in October. For this we inspect the life cycle~~ and ZMO3 runs, we examine the life cycles of upward propagating wave pulses entering the stratosphere ~~(represented by 100mb positive heat flux events) and how they differ between east and west QBO~~ during October, when the midlatitude QBO effect starts, and compare them between the two QBO phases. We take the strongest 30% of ~~100mb 80-45N~~ 100hPa 85-45N mean heat flux events~~for a given month~~[1], and divide them according to the phase of the QBO. ~~The time lag composites of anomalous $\overline{V'T'}$~~ Figure 5 shows heat flux pulses (Fig. 5a)~~and zonal mean zonal wind averaged over the extratropical stratosphere (85-40N, 50-0.1mb, marked by the green rectangle in Figure 6a) for October events~~[2] ~~show~~ , which induce a deceleration of the jet a few days after the peak 100hPa heat flux pulse (Fig. 5b), followed by an acceleration which partly reverses it. We see that while the heat flux pulses are ~~relatively~~ quite similar in magnitude and length~~(Fig. 5a), the deceleration of the jet is different between the QBO phases. Specifically, during both QBO phases, the life cycle shows deceleration followed by acceleration but the deceleration is stronger~~ , the wave induced deceleration is stronger, and the subsequent acceleration is weaker, during east QBO~~, and while in~~ . More specifically, during east QBO the ~~acceleration is smaller than the initial deceleration,~~ winds do not accelerate back to the values before the wave pulse, while during west QBO the acceleration completely reverses ~~it~~the deceleration, leaving the vortex ~~at~~ with similar strength. Since the anomalies are based on a climatology of the full run, we see part of the east-west QBO difference already at negative time lags, but this difference grows with each upward wave pulse. This is more clearly illustrated in latitude-height composites of the zonal mean zonal wind at different stages of the wave life cycle for east and west QBO phases (~~Figure~~ Fig. 6). The tropical QBO signal is evident, as well as a small but significant midlatitude QBO signal of opposite signs. This midlatitude signal is evident between 40-60N at all stages, even at negative time lags. During the peak of the event (days -3 to 3) we see a weakening of the zonal wind anomalies at high latitudes and all levels, but this weakening is much clearer during east QBO. At later stages, on the other hand, the winds strengthen back, essentially spreading the initial anomaly between 40-60N to polar latitudes. The strengthening of the midlatitude QBO signal over the life cycle is seen clearly when looking at the differences between the east and west composites (Figure 7c). To isolate the effect of the wave pulse from the preexisting QBO signal, we composite the zonal mean zonal wind time tendency (~~Figure~~ Fig. 7). We see a clear deceleration of the vortex during the peak of the event (days 3 to -3) for both QBO phases, with a slightly stronger deceleration during east QBO~~, but the~~ . The largest difference is during the end of the life cycle (days 7 to

[1] We only show results for positive heat flux events since we did not find negative heat flux events during October.

[2] ~~We only show results for positive heat flux events since we did not find negative heat flux events during October.~~

12)- while there is a very weak acceleration during east QBO, the acceleration is comparable in magnitude to the deceleration during west QBO.

To better understand the ~~zonal mean wind~~ polar vortex evolution we composite the zonal momentum budget (see Andrews et al. (1987), Eq.3.5.2a) (Figures 5c-5d). During east QBO events the deceleration is driven by a clear EP flux convergence which is counteracted by the Coriolis term, while during west QBO, these terms are much weaker. This is quantified more clearly by time integrating the different time tendency terms over the life cycle (days -10 to day 20, values indicated in the figure legend). In particular, the time integrated $\frac{d\bar{U}}{dt}$ represents the reversibility of the wave life cycle. In ~~the west QBO~~ particular, the positive value for the west QBO events (Fig. 5d) ~~events the positive value indicates the process is indeed~~ indicates the wave-induced deceleration is more reversible, while the negative value ~~in the east QBO composite~~ the the east QBO events (Fig. 5c) shows that a significant part of the wave-induced deceleration of the mean flow remains after the life cycle has ended.

To understand why the life cycle ~~is more reversible during~~ of west QBO events is more reversible we look at the latitude-height daily time lag ~~composits of EP-flux convergence~~ composites of EP flux divergence anomalies (Fig~~,~~. 8). There is stronger convergence (more negative values) at the high latitude upper stratosphere ~~in the~~ during east QBO events at days -3 to 7 (Fig. 8a, 8c) while ~~in the~~ during west QBO events, there is increased convergence in the subtropical region (Fig 8b, 8c). This suggests the waves propagate up along the polar vortex and break in the upper polar stratosphere during east QBO, while they refract equatorwards in the middle stratosphere during ~~the west QBOphase~~west QBO. This difference in wave propagation can be explained when examining the index of refraction ~~composites before the wave pulses start~~ just prior to the upward wave pulse events (days -5 to -10, Fig. 9). The index of refraction is stronger in the high latitude upper stratosphere during east QBO, and stronger in the midlatitude subtropics during west QBO~~,~~. A separation into vertical and meridional wavenubmers (c.f. Harnik and Lindzen (2001)) suggests the main contribution to these changes comes from the vertical wavenumber. This is consistent with the waves propagating to the upper polar stratosphere during east QBO and more equatorwards during west QBO. At later stages of the wave life cycle (days 8-17) ~~there are significant EP-flux divergence anomalies~~ during west QBO, there is a significant anomalous EP flux divergence, indicative of anomalous acceleration. This is consistent with a wavepacket trailing-edge acceleration~~which is~~ , expected to occur under non-acceleration conditions ~~which are satisfied when the waves are linear and damping is weak~~ of linear inviscid waves (Andrews et al., 1987). During east QBO, we see no such EP flux divergence region. This suggests the following picture: During fall, after the westerly winds get established and planetary waves start propagating up to the stratosphere, the waves are weak enough to be linear in the lower-mid stratosphere. Under these conditions, only waves which propagate up the polar vortex to the upper stratosphere/mesosphere grow enough (due to the density effect) to break nonlinearly. This happens during east QBO, and the deceleration induced by the breaking waves is irreversible in large part. During west QBO, the waves refract to the equator before reaching levels where they become significantly nonlinear, thus they decelerate the vortex when propagating up and accelerate it when refracting equatorwards. The strong acceleration is enabled due to non acceleration conditions being satisfied. ~~The strong acceleration is enabled due to non acceleration conditions being satisfied~~ [2]

[2]Strictly speaking, the non acceleration conditions apply ~~for~~ to the wave activity equation (the enstrophy equation divided by the PV gradient and density, so we are assuming the PV gradient is not zero over the domain and time periods we are examining. Also, non acceleration conditions apply ~~for~~ to a statistical

To explicitly examine the degree to which non-acceleration conditions are satisfied, we inspect the enstrophy budget and see how the different terms balance during these heat flux events. Following Equation 3 from Smith (1983) ~~we use~~for the enstrophy balance:

$$\frac{\partial}{\partial t}\frac{\overline{q'^2}}{2}\frac{\overline{q'^2}}{2} = -\overline{v'q'}\overline{q}_y - \overline{\frac{q'u'}{acos\phi}\frac{\partial q'}{\partial \lambda}} - \overline{\frac{q'v'}{a}\frac{\partial q'}{\partial \phi}} + \overline{q'D'_{sw}} + \overline{q'D'_{lw}} - Resid \quad (1)$$

~~where~~

$$D' = \frac{Rf}{H\rho}\frac{\partial}{\partial z}\frac{\rho Q'}{N^2}$$

~~where X' denotes~~ Primes denote the deviation from the zonal mean~~and~~ , q is the QG potential vorticity, and D' is the temperature time tendency from diabatic heating:

$$D' = \frac{Rf}{H\rho}\frac{\partial}{\partial z}\frac{\rho Q'}{N^2} \quad (2)$$

where Q' is the temperature time tendency from radiation, both short and long wave. On the right hand-side of Eq. 1, the first term is the wave-mean flow interaction~~term~~, equivalent to the ~~EP-flux~~ EP flux divergence times the meridional gradient of the zonal mean potential vorticity ($\overline{q}_y$), the second and third terms are the non-linear terms, the fourth and fifth terms are the diabatic terms from shortwave and longwave radiation~~(where Q' = temperature tendency from shortwave or longwave radiation)~~ , and the last term is the residual of the total time tendency minus all the terms on the right hand side. Large nonlinear, damping and residual terms indicate a violation of non-acceleration conditions (Andrews et al., 1987).

~~To avoid misinterpreting the differences in the enstrophy balance we normalize the events by the mean value of the heat flux amplitude entering the stratosphere at the peak of the events between day −3 and 3 ($\overline{V'T'}$ at 100mb).~~ Figure 10 shows the time-lagged composites of the different enstrophy budget terms of Eq. 1, averaged over 40-70N, 50-1mb. The averaging area was chosen based on an examination of latitude-height composites. ~~As expected, the nonlinear terms (red line in Fig. 10a) are larger~~ We see that during both QBO phases, the enstrophy time tendency (blue lines in Figures 10) is driven by the linear term (black lines in Figures 10), and slightly damped by thermal damping (magenta lines in Figures 10), but the nonlinear (red lines in Figures 10) and residual terms (gray lines in Figures 10) are large and significant during east QBO, ~~while~~ and are much smaller during west QBO~~events the wave transience term is more significant (black line in Fig. 10b). The results are~~ . This is consistent with White et al. (2016) who used reanalysis data to study the different seasonal cycles between east ~~/~~and west QBO, and found that non-linear interactions are stronger ~~for~~ during Nov-Jan of east QBO years~~during Nov-Jan.~~

steady state. Here we are interested in the net deceleration over the wave life cycle, and can assume quite safely that the time averaged (over the wave life cycle) enstrophy time tendency vanishes over the wave life cycle.

~~To~~ . These results suggest that the dynamics during west QBO are more reversible (closer to non acceleration). We note, however, that during east QBO, the nonlinear terms act to reduce wave enstrophy, while the residual acts to increase it. The cancellation is quite large, and in fact, the sum of the nonlinear and residual terms gives a slightly negative value which is only slightly more negative during east QBO. The residual terms, however, are very noisy, while the nonlinear terms have a coherent spatial structure, so that this cancellation only occurs when we take a latitude-height average. The large residual may be an artifact of our having daily, rather than shorter time scale output, and further examination is needed to better understand the role of ~~ozone waves we repeat the analysis shown in Figure 8~~ nonlinearities.

We now turn to examining the role of ozone waves, by repeating the analysis for the ZMO3 run. ~~The results are shown in Figure 11~~ Figure 11 shows the time-lagged composites of the EP flux and its divergence (compare to Figure 8). The main point to note is the lack of strong ~~positive anomalies~~ anomalous EP flux convergence at positive time lags during west QBO, ~~suggesting the wave induced deceleration is not as reversible as in the~~ which for the 3DO3 run made the west QBO wave-induced deceleration reversible. This weaker trailing-edge ~~deceleration~~ acceleration for the ZMO3 run is consistent with ~~there being~~ a stronger radiative damping of the waves in the lower-mid stratosphere ~~.~~ as a result of removing the tendency of ozone waves to weaken the radiative damping in these regions (Fig. 1c). In addition, ~~we see~~ during east QBO, there is weaker EP flux divergence ~~compared to the 3DO3 run for east QBO at~~ in the upper stratosphere on days 4 to 7, consistent with ~~ozone waves increasing the upper stratospheric wave damping .~~ a weaker wave damping as a result of removing the tendency of ozone waves to increase radiative damping there (Fig. 1c).

The above results suggest that ozone waves affect the total wave-life cycle mean EP flux divergence in ~~opposite manners during~~ an opposite sense between east and west QBO phases - they decrease it during west QBO and increase it during east QBO. A closer examination ~~of the EP flux in our runs shows the vertical EP flux is strongly converging while the meridional EP flux is strongly diverging (not shown). Figure 12 shows the difference between 3DO3 and ZMO3 runs of the latitude-height composites during the later stages~~ shows that this is due to the differences in wave propagation and damping patterns, which causes the ozone wave damping to affect the EP flux divergence during different times of the wave life cycle ~~(days 4 to 7 and for days 8 to 11), for east~~ (during the two QBO phases (Fig. 12~~a)and west (Fig. 12b) QBO. We find that both the vertical convergence and the meridional divergence are~~). During east QBO, the EP flux divergence is stronger in the upper stratosphere during the peak of the deceleration (days 4-7) in the 3DO3 ~~run compared to the ZMO3 run (not shown)~~ run, consistent with the waves being damped more strongly in the upper stratosphere. During west QBO, ~~but while during east QBO phase the vertical convergence on days 4 to 7 dominates the EP flux divergence (Fig. 12a), during west QBOphase, the meridional convergence on days 8 to 11 dominates the EP flux divergence (Fig. 12b). This results in more EP flux~~ there is a significant EP flux anomalous convergence in the ~~3DO3 run during east QBO and more EP flux divergence~~ upper stratosphere at late stages of the life cycle in the 3DO3 run~~during west QBO. Correspondingly the vortex is weaker in the 3DO3 runduring east QBO and stronger during west QBO~~, which is absent in the ZMO3 run, consistent with a weaker ozone-induced damping strengthening the trailing edge effect.

~~The results shown so far were for October. The differences in individual life cycles lead to a slightly stronger deceleration and warming of the polar vortex during east QBO compared to west QBO phases. Similar differences are also found in November.~~

~~These differences~~ Besides a difference due to changes in wave propagation pattern, it is also possible that the short wave thermal forcing itself varies between east and west QBO~~cycles continue and are thus further intensified later in November (not shown), so that by early winter the polar vortex is weaker~~ , due to changes in the amplitude of ozone waves and the correlations between ozone and temperature anomalies. An examination of the wave 1 ozone budget shows weaker ozone waves during east QBO~~years compared to WQBO years (Fig. 4a). We also find a stronger poleward meridional circulation in the subtropical lower stratosphere, which extends to higher levels and latitudes at positive time lags (not shown). These results are consistent with Garfinkel et al. (2012) though they used a different model configuration (WACCM version 3.1 with fixed SSTs and perpetual winter radiative forcing, compared to our freely running model with interactive ocean and sea ice components version).~~

~~The radiative effects of ozone waves, which are strongest in fall (Table 3, 1st and second column) cause the stronger vertical and meridional convergence, which dominate the EP-flux convergence differently under the different QBO phases and cause the stronger deceleration in the east QBO phase and stronger recovery in the west QBOphase, resulting in the earlier Holton-Tan effect seen in the 3DO3 run. Kodera and Kuroda (2002) found that solar cycle variations have the largest influence on stratospheric winds in the transition period between the time when the stratosphere is radiatively controlled (early winter) and~~ , due to weaker meridional gradients of zonal mean ozone during east QBO. This weakening of the ozone waves is accompanied by a reduction of the short-wave damping in the lower to mid stratosphere, and a strengthening of the total radiative wave damping. The temperature wave amplitude, however, is still stronger during east QBO, suggesting the effect of changes in zonal mean ozone gradients are of second order.

3.4 The subsequent seasonal evolution of ozone-wave effects

As seen in section 3.1, the ~~time when it is dynamically controlled by wave-mean flow interactions (late winter). Interestingly, we also find that ozone wave effects, which one might consider to be another mechanism through which anomalies in solar heating affect the stratosphere, have the largest impact during the transition period which occurs in our model in November. The transition period was identified by examination of the zonal mean temperature time tendency, which was either controlled by the tendency from radiation or dynamics~~ direct radiative ozone-wave effect starts very early on in September, when the waves just emerge from the troposphere and are not yet affected by the phase of the QBO. The main effect is to increase the EP flux convergence in the upper stratosphere (Fig. 3c) and slightly weaken the vortex (Fig. 3c). During October, when the waves grow a bit, we see that individual wave life cycles are significantly affected by the phase of the QBO, so that the wave induced deceleration is slightly stronger during east QBO compared to west QBO. The ozone-wave radiative interaction affects individual life cycles in an opposing manner between east and west QBO phases, which strengthens the east-west QBO differences. This was shown explicitly only for October life cycles, but we find similar life cycle behavior during November as well. As a result, the stronger EP flux convergence during east QBO strengthens and descends lower down as the winter evolves (not shown)~~.~~ , resulting in a weaker polar vortex by November during east QBO years (Fig. 13a, green line).

~~Finally, we look at the seasonal differences in the development between the 3DO3 and ZMO3 runs at each QBO phase separately, where the phase of~~ Later in the winter, the waves become stronger and more nonlinear, and short wave radiation

decreases. As a result, the direct effect of ozone waves is strongly reduced and a modulation of wave-mean flow interaction takes over the midlatitude QBO signal, in the form of a polar night jet oscillation (Kuroda and Kodera, 2001), which arises because changes in the vortex strength affect the strength of the waves and their induced deceleration, while changes in the waves affect their deceleration of the vortex. This is evident from Figure 13, which shows the ~~QBO for the entire winter season is defined in October. Figure 13 shown the~~ daily climatology ~~of~~ and the interannual range of the EP flux divergence, integrated over 85-45N and 10-0.1hPa, for the ~~EP-flux divergencein the~~ 3DO3 (black) and ZMO3 (blue) runs and ~~the~~ their difference (red)~~, and the zonal mean zonal wind differences~~ . Also shown is the difference in the vortex-integrated zonal mean wind for 3DO3 minus ZMO3 runs (green)~~in~~ , for east (Fig. 13a) and west (Fig. 13b) QBO years~~, averaged over 85-45N and 10-0.1hPa. As seen in Section 3.1, influence of the direct ozone wave effect starts with increased EP-flux convergence in the upper stratosphere during September(Fig. 3c). The increased convergence strengthens and descends lower down resulting in a weaker polar vortex by November during east QBO years (Fig. 13a, green line). This initiates a~~ . We see the ozone wave influence described in the previous two sections - a very small but significant weakening of the vortex for 3DO3 compared to ZMO3 for both QBO phases during September, which strengthens in October for the east QBO but reverses sign in October of west QBO. This preconditioning of the winter vortex initiates an oscillation between the anomalies of EP flux divergence and zonal mean zonal wind, similar to that which gives rise to the *polar night jet oscillation* ~~*in mid winter due to a preconditioning of the vortex: less upward wave propagation and deceleration (in Nov-Dec), followed by a stronger vortex*~~ (Kuroda and Kodera, 2001): less wave-induced deceleration leads to a weaker jet, which in turn reduces the amount of waves propagating up the vortex, allowing the vortex to strengthen from mid-December~~, although the signal is~~ . We note, however, that although the anomalies in EP flux divergence and zonal mean winds are much larger during mid winter compared to fall, they are not statistically significant ~~due to the noisy winter resulting of inter-annual variability~~ over most of the winter (Fig. 13a, red and green lines). ~~In addition, we find differences in the zonal mean ozone concentrations in the polar region starting in September of around 6-8% in the high latitude mid stratosphere (not shown). We note that in a previous study by Albers et al. (2013) it was mentioned that the zonal mean ozone variations were negligible. In our study, we do find these small differences to be statistically significant, and inspecting the zonal mean tendency from shortwave heating show these effects can reach up to 10% of the climatological time tendency in early winter ($0.05\frac{K}{day}$ in Sep-Oct), however, they are much weaker later in mid winter (not shown). These changes can also invite additional feedbacks on the ozone wave radiative effects through modulation of the ozone wave amplitudes.~~

~~In the west QBOyears,~~ This is due to the large interannual variability (wide grey shading region), and the ~~apparent opposite effect of the ozone waves on the EP-flux convergence is due to the reversible life-cycle of upward propagating wave events starting earlier in winter which allows~~ occurrence of occasional sudden stratospheric warmings. During west QBO, these cycles start in the opposite phase compared to east QBO, with stronger EP flux divergence, followed by a stronger vortex~~by December in the 3DO3 run~~ , which is followed by more waves propagating up the vortex, and subsequent deceleration (Fig. 13b, red and green lines). ~~The latter allows enhanced wave propagation (also accompanied by overall stronger wave pulses entering the stratosphere) and then deceleration of the flow in January (Fig. 13b).~~ These induced changes in the circulation cause a dynamical cooling (heating) during December (January) in the lower stratosphere, and heating (cooling) during December (January) in the upper stratosphere/lower mesosphere (not shown). ~~When considering all 100 years of the model runs, the~~

response to ozone wave radiative effects We note that only the latter part of the cycle is statistically significant, suggesting the radiative effects of ozone waves are less robust during west, compared to the east QBO, with the most robust signal showing up in their difference.

We also find statistically significant 3DO3-ZMO3 anomalies of zonal mean ozone concentration, of about 6-8% in the polar mid-stratosphere, starting from September (not shown). Consistently, the zonal mean short-wave radiation heating anomalies reach up to 10% of the climatological time tendency in early winter ($0.05\frac{K}{day}$ in Dec-Jan is missing (see the lack of statistically significant signal during these months in Figure 2)as a result of them being of opposite sign during these months in east and west QBO phases (Fig. 13, green line). Sep-Oct), though they are much weaker later in mid winter (not shown). These changes are much weaker in the west QBO phase (about half the magnitude) during October, and are not statistically significant during November. These changes may feedback on the ozone wave radiative effects through modulation of the ozone wave amplitudes, and might be an additional cause to the east-west QBO differences in the winter march. This is different from the Albers et al. (2013), who noted that zonal mean ozone variations were negligible.

4 Conclusions

The direct radiative effect In this study we examined the radiative effects of ozone waves is studied using the WACCM modelon the midlatitude polar vortex, using a set of WACCM model runs in which a control simulation with a nudged QBO is compared to a run where only the zonal mean part of the ozone field is passed on to the radiative heating code. We find these effects can be important in early winter when the polar night jet is formed and there is still enough radiation where the ozone and temperature waves are relatively stronga weak but significant effect during September, when the westerly polar vortex just starts getting established, which is not dependent on the phase of the QBO (Fig. 3).

Later on, in October, ozone wave heating affects the life cycles of upward propagating waves, and since the wave life cycle is different for east and west QBO, the ozone wave effect is also different, and opposite. As a resultthere is an increase in the mean flow deceleration from wave absorption in the upper stratosphere in the , it is only significant when considering each QBO phase separately (Fig. 4). Moreover, in the 3DO3 run, while decreasing it in the lower stratosphere (September, see Figure 3c). The acceleration/deceleration pattern has a poleward tilt, effectively confining the polar winter jet to higher latitudes the mid-latitude effect of the QBO starts earlier in the season, in October, compared to December in the ZMO3 run (Fig. 3d4). This helps to focus the waves to the higher latitudes and as a result a stronger deceleration of the winds (McIntyre, 1982) in the following months. This happens due to weaker wave damping on temperature waves in the lower stratosphere and stronger damping in the upper stratosphere, as expected by earlier theoretical studies. These short-wave radiative influence of the waves only occurs during fall when the waves are still weak (compared to mid winter) and radiation is still strong, yet the individual wave life cycle effects accumulate to affect the a significant preconditioning which influences the subsequent development of the mid winter polar jet. While we find

It is interesting to compare our results to previous studies. We find that ozone waves weaken the zonal mean winds to weaken until November, (McCormack et al., 2009) found a response in mid winter: mid-Jan to February. However, their

experiment was run for Dec-Mar with similar initial conditions. Our most robustly during fall (with a peak in November (Fig. 2). These results are consistent with those of Gillett et al. (2009) who found the weakening to occur earlier in October to mid-December, and they an ozone-wave induced weakening during October to December. McCormack et al. (2009), on the other hand found a response in January - February, however, they ran a pair (an ensemble of pairs) of Dec-Mar simulations with similar initial conditions, while Gillett et al. (2009) used a 40-year simulation of the entire seasonal cycle, and their model has a realistic QBO which is spontaneously produced (Scinocca et al., 2008), thus having more resemblance to our model setup. A possible explanation to these discrepancies between McCormack et al. (2009) to Gillett et al. (2009) and our results is with a spontaneously produced realistic QBO in their model (Scinocca et al., 2008). This suggests the inclusion of the a full seasonal cycle , which makes the differences appear in early winter and the late winter signal then becomes too noisy, while in starting the allows the ozone-wave influence to appear in fall, and to be less significant later in the winter when internal variability takes over. Moreover, the existence of a realistic QBO in our runs masks the signal in mid-winter if the analysis is done averaging both QBO phases together (it will be interesting to see how the analysis of Gillett et al. (2009) would change if the results are stratified by the phase of the QBO). Starting the simulation in mid winter (Dec), when radiation is still weak at high latitudes, with similar initial conditions helps to for the 3DO3 and ZMO3 runs (as in McCormack et al. (2009)), helps get a cleaner ozone-wave signal in late winter. The existence of a realistic QBO can also explain this as we saw the apparent opposite effect of ozone waveson east/west QBO can mask the signal in mid-winter. It can be insightful to repeat the analysis of Gillett et al. (2009) considering the phase of the QBO and see how our results apply to other climate models. , despite the weaker short-wave radiation and stronger waves. It is also interesting to compare our results to the more simplified 1D model Nathan and Cordero (2007) used for mid-winter conditions. Their results are most comparable to our results during fall (September) - they found decreased EP flux convergence in the lower stratosphere where ozone waves reduce the radiative damping on temperature waves (they find a reduction of $\tilde{2}5\%$ while we find $\tilde{1}0\%$), and an increase in EP flux convergence is two times stronger in the upper stratosphere where ozone waves increase the radiative damping (while we find $\tilde{1}0\%$).

We further found that the effects of ozone waves depend The dependence of the radiative ozone-wave effects on the phase of the QBO in early winter . A synoptic analysis of east /west QBO differences in early winter is used to understand the mechanism to explain this. The events of upward wave propagation behave differently. The life cycle of the west QBO events during early winter was examined by compositing individual wave life cycles during October, for east and west QBO separately. We find that the life cycle during west QBO is more reversible in early winter (Fig. 5d), and allowing the polar night jet can recover after to recover from the deceleration which an upward propagating wave events pulse induces (Fig. 5b). These differences in the individual The small differences of single wave events add up, and the cumulative effect is consistent with the known Holton-Tan effect resulting in a stronger polar vortex in during west QBO years, which . We further showed that this difference occurs a month earlier in the 3DO3 run (Fig. 4). In the east QBO events there is stronger EP-flux convergence at the upper levels (Fig 8a), which is further increased in the 3DO3 run in early winter, and as . As winter progresses the deceleration is extended poleward and downward. The ozone waves increase both meridional and vertical convergence of the EP-flux in early winter (Fig. 12), however, they are opposite in sign at higher latitudes, and in the west QBO phase the meridional part is more dominant at positive time lags. This causes the weaker deceleration During west QBO, ozone waves weaken the wave

damping in the lower stratosphere, render the dynamics more reversible. In particular, the acceleration at the trailing edge of the wavesresponsible for the reversibilityof the west QBO events to appears a month earlier , which is responsible for this reversibility, is stronger in the 3DO3 run, and resulting in the resulting in an earlier Holton-Tan signal. Our model setup used fixed GHGs and ODSs at 1960's levels, where ozone waves are weaker compared to the 1990's (not shown). It is possible that the ozone wave effects found in this study will be much stronger under climate change conditions and will have a larger impact on the inter-annual variability.

The analysisprovided for the life cycle of wave events at This synoptic-type life cycle analysis, done separately for the different QBO phases, provides an additional mechanism to understand the Holton-Tan effect. In particular, the influence of ozone wave effects might For example, Watson and Gray (2014) did not find a fall-early winter Holton-Tan effect (as is found in the observations). While they suggest their delayed response has to do with the response time scale to tropical wind anomalies, it is also possible that their use of zonal mean ozone in the radiative code of their model also contributes to this delay. It is not clear, however, if the strengthening of the Holton-Tan effect by ozone waves is unique to our model, or if it holds for other models as well. It is also possible that a lack of ozone wave effects may explain the weak Holton-Tan effect produced by climate models forecasts forecast models (Smith et al., 2016), and might improve the predictability if included (Scaife et al., 2014).

Previous studies showed the relationship between solar cycle effects through modulation of the tropical stratospheric ozone heating affect the high latitude polar vortex depending on the phase of the QBO Our results may also help understand the influence of the 11-year solar cycle on the polar vortex, and its dependence on the QBO phase (eg. Labitzke and Van Loon (1988), Garfinkel et al. (2015)). Our result provide an additional mechanism through which solar cycle effects might play a role in the circulation of the stratosphere (through modulating the direct For example, it is possible that the solar cycle modulates the strength of the ozone-wave radiative forcing.

Finally, our model setup used fixed GHGs and ODSs at 1960's levels. Under this configuration, ozone waves are weaker compared to the 1990's (not shown), thus we expect the ozone wave effects on the temperature waves) and their sensitivity to the tropical stratospheric winds, and requires further study. to be stronger in runs with present day forcings, and it remains to be examined how these effects might change in the future.

5 Tables

Table 1. ~~Model~~ The model setup for the 3DO3 and ZMO3 experiments

Experiment	QBO	SST/Sea Ice	Ozone passed to radiation code
3DO3	nudged	interactive	Full field
ZMO3	nudged	interactive	Zonally averaged

Table 2. ~~Number~~ The number of positive heat flux events ~~for~~ during east ~~/~~and west QBO ~~phase~~ phases, for Oct-Dec~~for~~ , in the 3DO3 and ~~the~~ ZMO3 experiments.

Month	EQBO(3D)	WQBO(3D)	EQBO(ZM)	WQBO(ZM)
Oct	55	46	44	43
Nov	52	48	44	35
Dec	52	39	47	38

Table 3. ~~Showing the~~ The seasonal development (Oct-Dec) of the integrated values of the following: $\frac{\int f(|T|)\cdot|T|dydz}{\int|T|dydz}$, where $f(|T|) = \frac{d|T|_{tend1}}{d|T|_{tend2}}$, and tend1 and tend2 ~~are~~ denote two different time tendency terms for the ~~temperature~~ wave 1 temperature amplitude~~tendencies from short-wave/long-wave radiation and from dynamics~~, averaged over 80-40N, 50-0.5mb, for the 3DO3 run. The terms shown are the time tendency terms due to short-wave and long-wave radiation, and dynamics.

Month	$\frac{swr}{lwr}$	$\frac{swr}{dyn}$	$\frac{rad}{dyn}$	$\frac{lwr}{dyn}$
Sep	~~0.1438~~ 0.37	~~0.0813~~ 0.185	~~0.1552~~ 0.3582	~~0.1865~~0.4499
Oct	~~0.1897~~ 0.175	~~0.0882~~ 0.086	~~0.3918~~ 0.3822	~~0.4458~~0.4356
Nov	~~0.0997~~ 0.09	~~0.0481~~ 0.046	~~0.4598~~ 0.4693	~~0.4875~~0.4971
Dec	~~0.0663~~ 0.058	~~0.0286~~ 0.0283	~~0.4407~~ 0.4645	~~0.4532~~0.4771

6 Figures

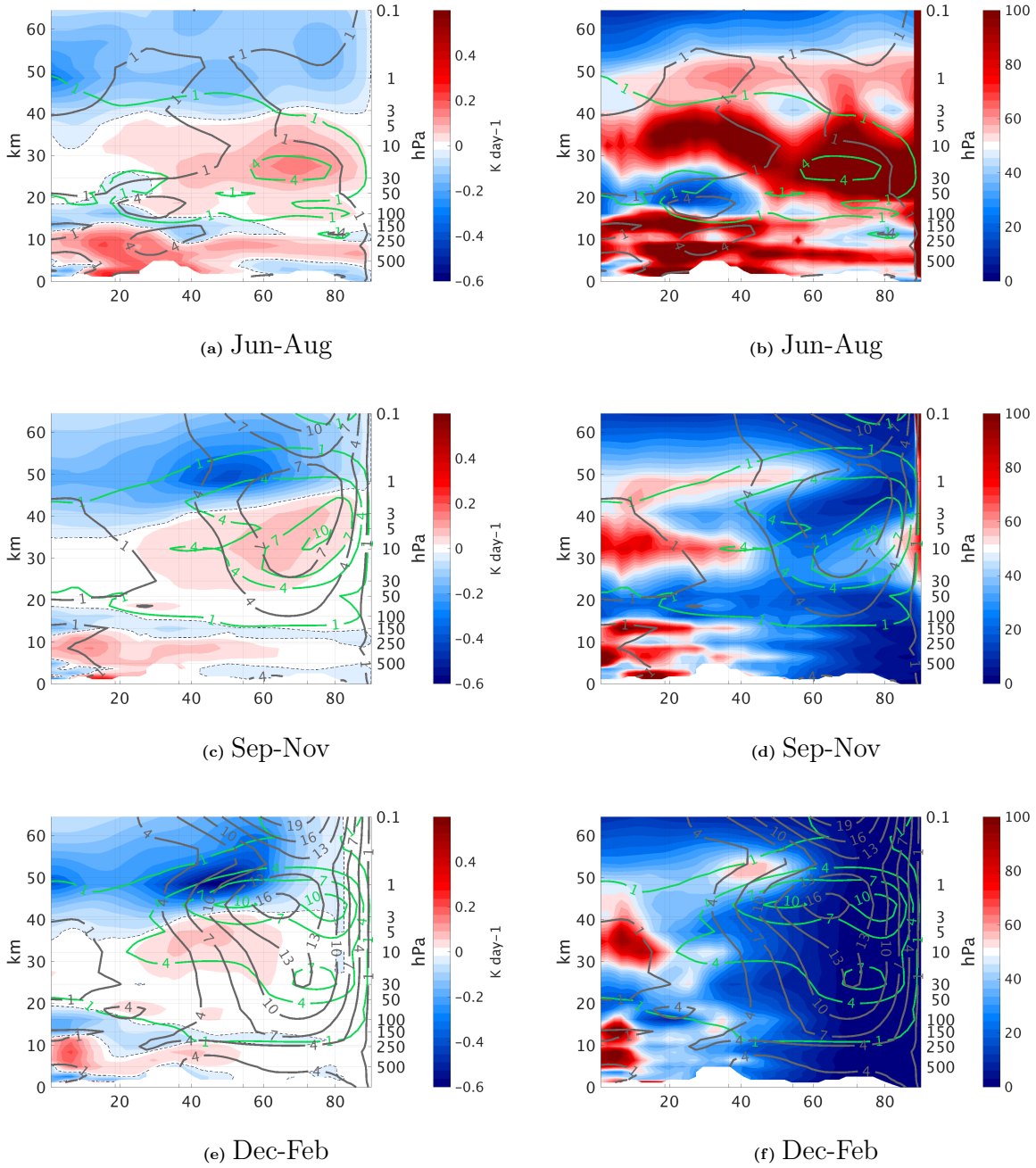

Figure 1. Monthly mean temperature tendency from SWR of temperature zonal wave 1 amplitude (left), $\%\frac{SWR}{LWR}$ (fraction of the tendency from SWR of temperature zonal wave 1 amplitude compared to LWR (right), in the ~~northern hemisphere~~ Northern Hemisphere during Jun-Aug (top), Oct-Nov (mid) and Dec-Feb (bot). Temperature (ozone) wave 1 amplitude in K ($10^{-7}\frac{kg}{kg}$) are shown in gray (green) contours.

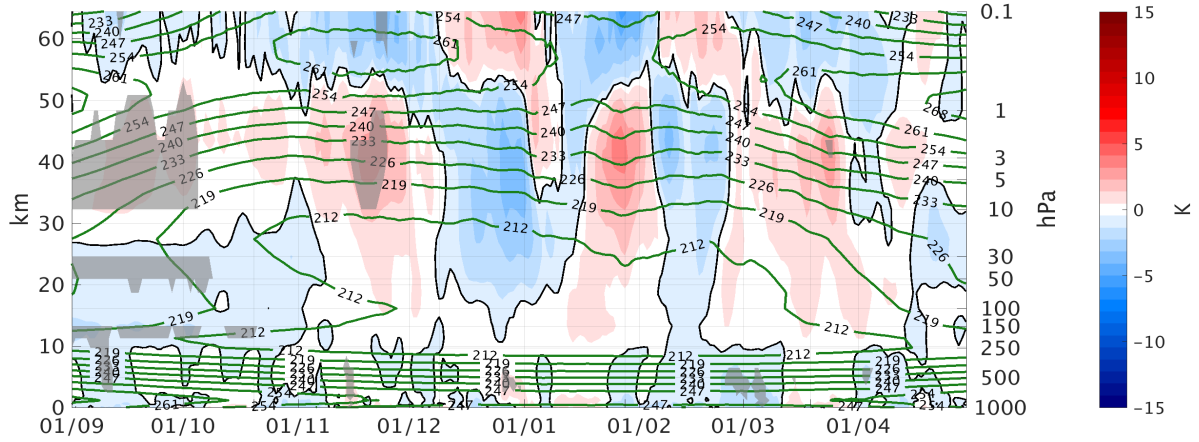

(a) Tzm (90-60N) 3D-ZM

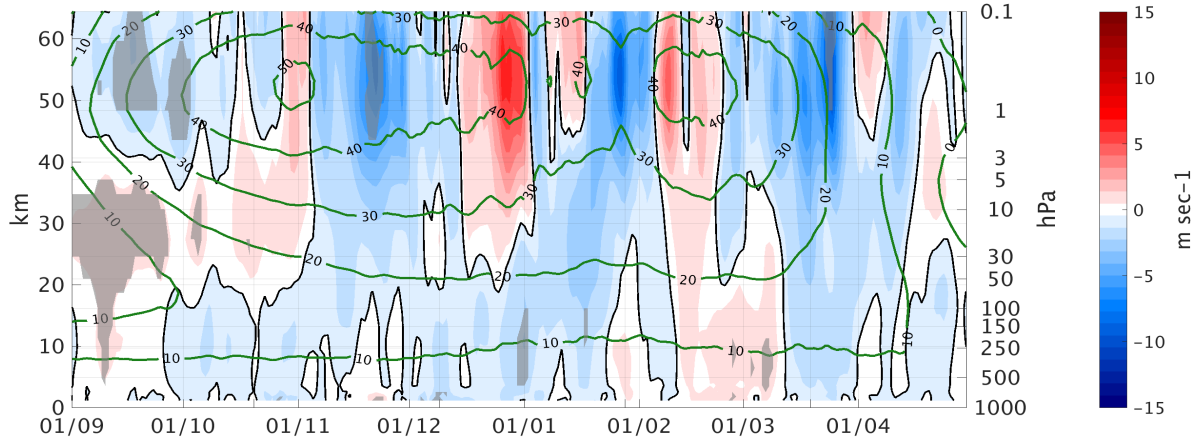

(b) Uzm (75-55N) 3D-ZM

Figure 2. Height-time differences between the 3DO3 and ZMO3 run for all years for zonal mean temperature, zonal wind, ~~EP flux~~ EP flux divergence, and temperature zonal wave 1 amplitude (from top to bottom). The difference between the 3DO3 and the ZMO3 model runs are indicated by the colored contours, the climatology of the 3DO3 run is shown by the green contours. Statistically significant areas are shown by gray shading.

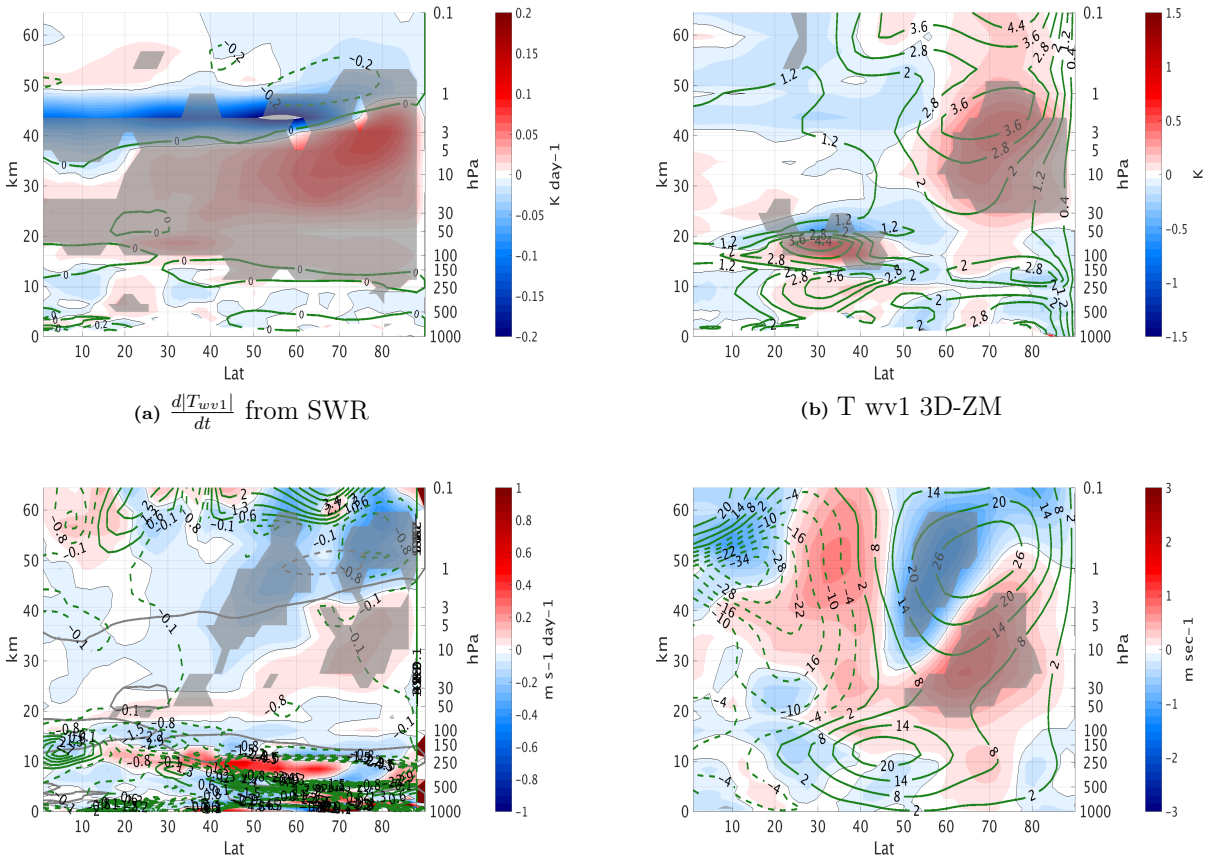

(a) $\frac{d|T_{wv1}|}{dt}$ from SWR

(b) T wv1 3D-ZM

(c) EPFD 3DO3-ZMO3

(d) Uzm 3D-ZM

Figure 3. September mean differences between the 3DO3 and ZMO3 run for all years for temperature wave 1 amplitude tendency from short-wave radiation (3a), temperature zonal wave 1 amplitude (3b), ~~EP-flux~~ EP flux divergence (3c), and zonal wind (3d) . In Figure 3c the gray line in the upper stratosphere ~~indicated~~ indicates the height where ozone and temperature zonal wave 1 correlation change from positive to negative. Statistically significant areas are shown by gray shading.

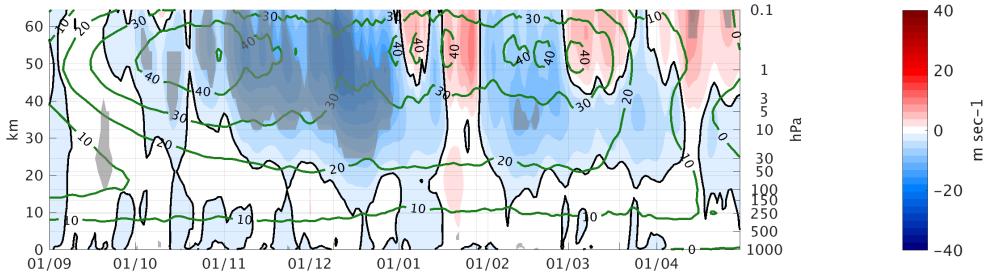

(a) Uzm EQBO-WQBO 3DO3

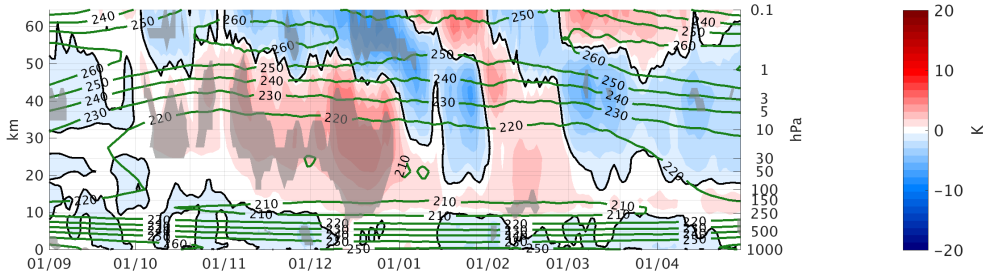

(b) Tzm EQBO-WQBO 3DO3

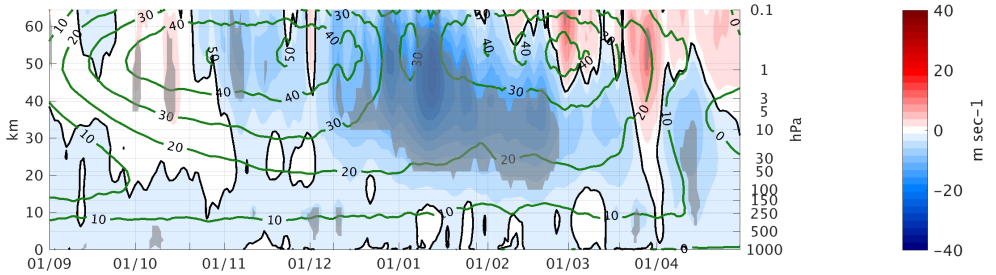

(c) Uzm EQBO-WQBO ZMO3

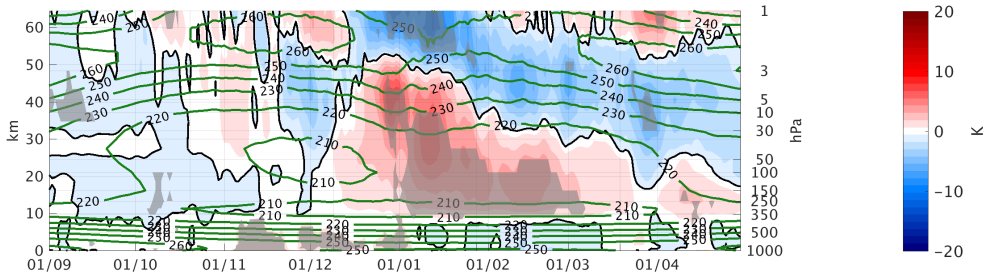

(d) Tzm EQBO-WQBO ZMO3

Figure 4. Daily climatology differences between east and west QBO phase of the zonal mean zonal mean zonal wind averaged over 75-55N for the 3DO3 (4a) and ZMO3 (4c) runs, and the zonal mean temperature averaged over 90-66N for the 3DO3 (4b) and ZMO3 (4d) runs, for Sep-Mar. Statistically significant areas are shown by gray shading.

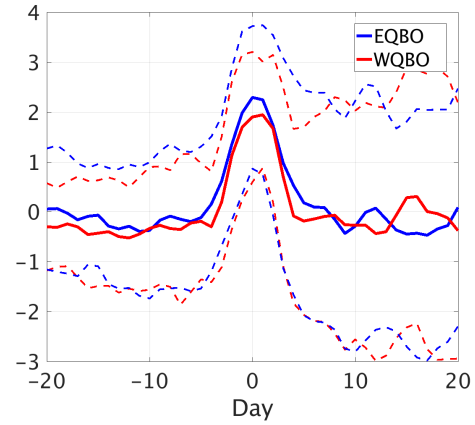

(a) $\overline{V'T}$ ($\frac{m \cdot K}{sec}$), 100mb, 85-45N

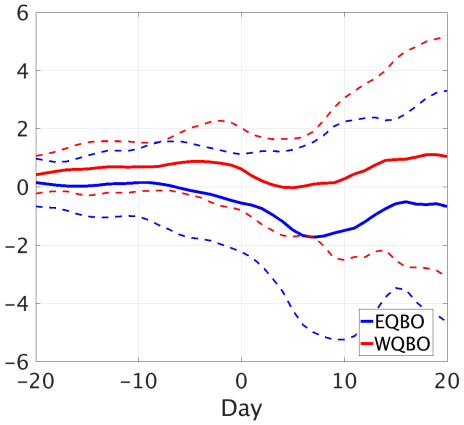

(b) $\overline{U}$ ($\frac{m}{sec}$), 50-0.1mb, 85-40N

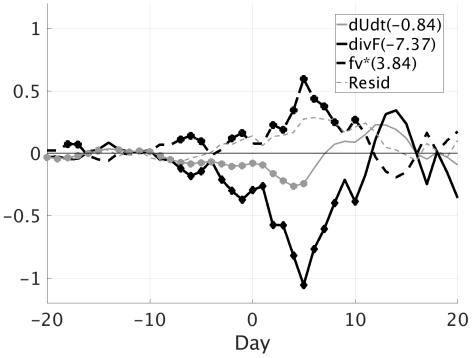

(c) Momentum Budget ($\frac{m}{sec \cdot day}$), 50-0.1mb, EQBO

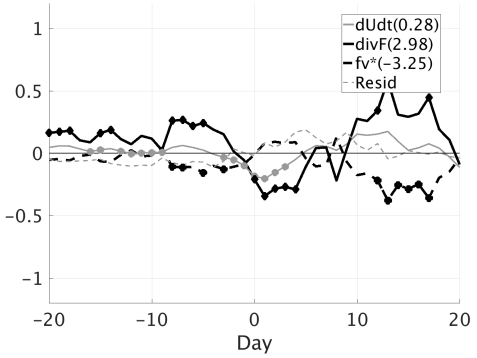

(d) Momentum Budget ($\frac{m}{sec \cdot day}$), 50-0.1mb, WQBO

Figure 5. Time lag composites for the upward wave pulse events during October in the 3DO3 run. (a) $\overline{V'T'}$ averaged over 85-45N at 100mb. (b-d) The extratropical stratospheric averages (50-0.1mb, 85-40N, marked by the green rectangle in 6a))of: (b) $\overline{U}$, dashed lines show ± 1 standard deviation. (c-d) Momentum budget terms for east and west QBO events respectively. Shown are the total time tendency (thin gray), $f\overline{v}^*$ (dashed black) and the residual (gray dashed) with their integrated value from day -10 to 20 denoted in the figure legend.

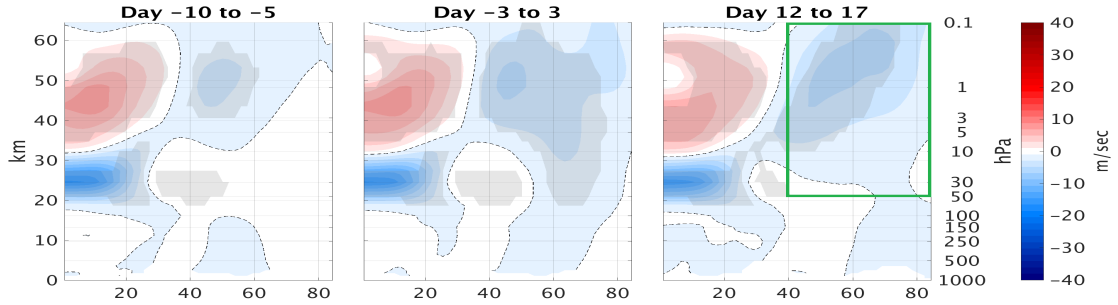

(a) $\overline{U}$, EQBO, 3DO3

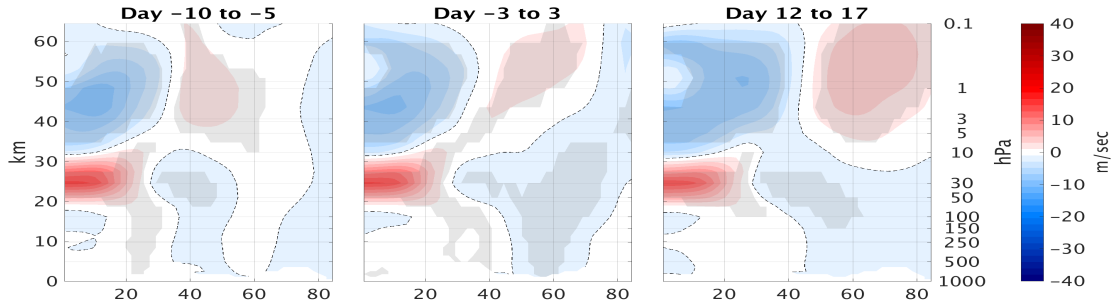

(b) $\overline{U}$, WQBO, 3DO3

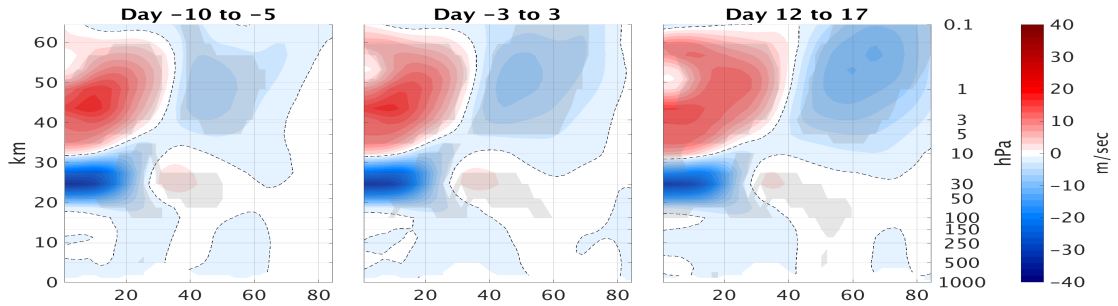

(c) $\overline{U}$, (E-W)QBO, 3DO3

Figure 6. Time lag composit of the zonal mean zonal wind anomalies for east QBO (6a), west QBO (6b), and the difference between them (6c), for the positive heat flux events from the 3DO3 run of October. The green box in Figure 6a shows the area of averaging for Figures 5b-5d.

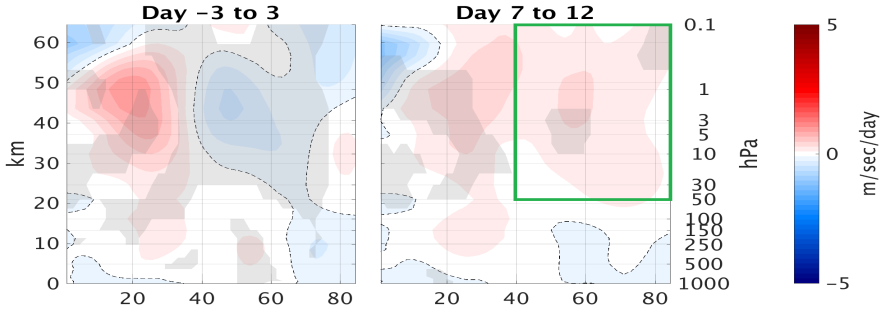

(a) $\frac{d\overline{U}}{dt}$, EQBO, 3DO3

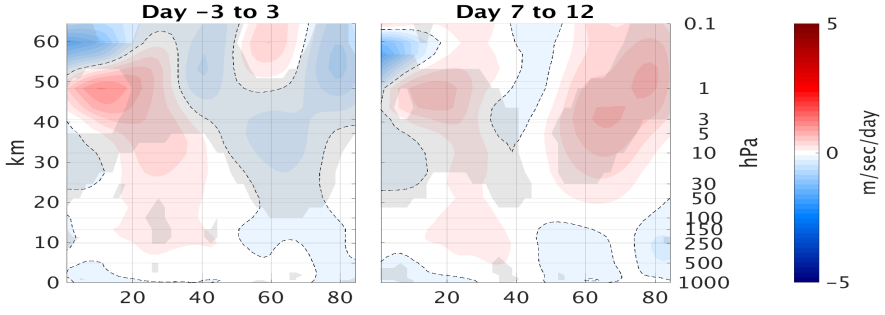

(b) $\frac{d\overline{U}}{dt}$, WQBO, 3DO3

Figure 7. Time lag composit of the zonal mean zonal wind time tendency for east QBO (7a) and west QBO (7b), for the positive heat flux events from the 3DO3 run of October. The green box in Figure 7a shows the area of averaging for Figures 5b-5d.

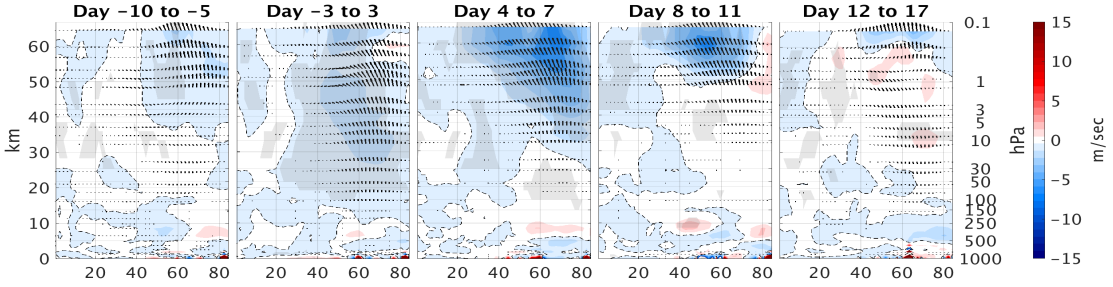

(a) Oct, $\nabla \cdot F$, EQBO 3DO3

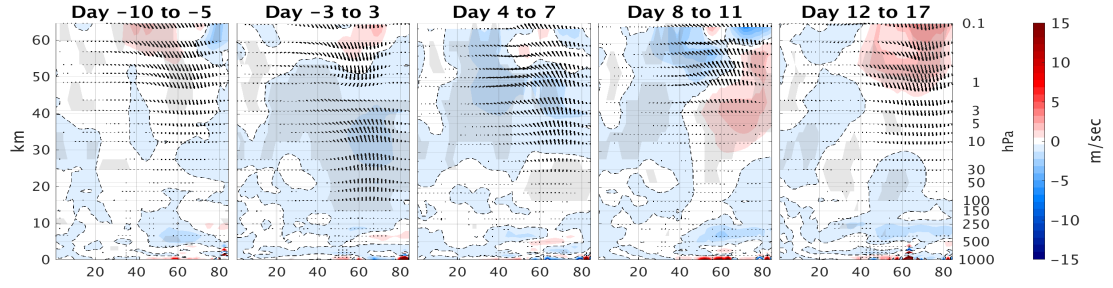

(b) Oct, $\nabla \cdot F$, WQBO 3DO3

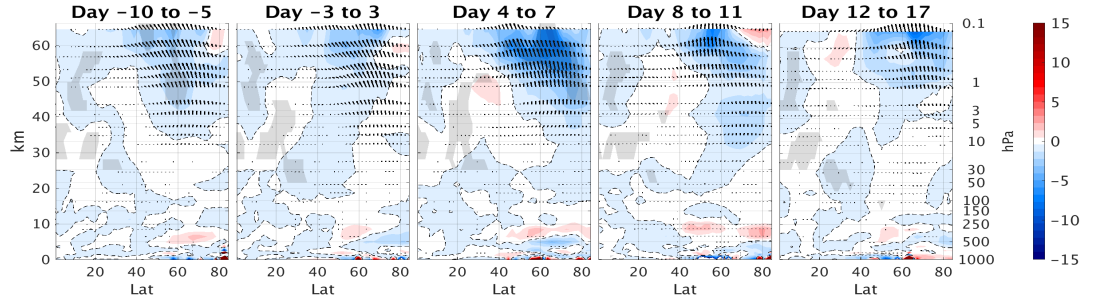

(c) Oct, $\nabla \cdot F$, (E-W)QBO 3DO3

Figure 8. ~~Lat-height~~ Latitude-height time lag ~~composits~~ composites of ~~EP-flux~~ EP flux divergence (anomalies from the climatology) for the positive heat flux events (70th percentile of $\overline{V'T'}$ at 100mb 85-45N), for east (8a), west (8b) and the their differences (8c) for October events for the 3DO3 run. Statistically significant areas are shown by gray shading.

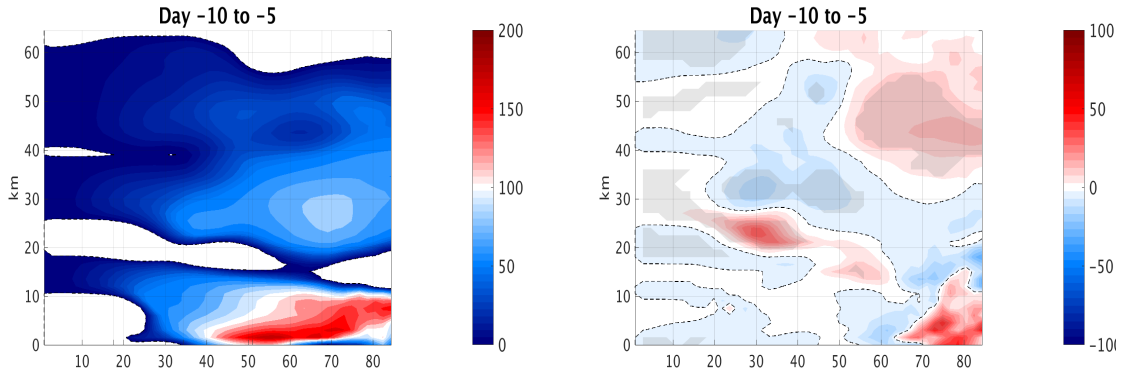

(a) n EQBO

(b) n^2, (E-W)QBO

Figure 9. Index of refraction ~~$(n^2 = \frac{N^2}{f_o^2}\frac{\bar{q}_y}{\bar{U}-c} - k^2\frac{N^2}{f^2} + F(N^2)\frac{N^2}{f^2})$~~ $\left(n^2 = N^2\left[\frac{a\bar{q}_y}{\bar{U}-c} - \frac{s^2}{a^2\cos^2\phi} + a^2 f^2 F(N^2)\right]\right)$, see eq. ~~5~~ C2, ~~6~~ 5 in Harnik and Lindzen (2001))at days -10 to -5 for (a) east QBO, and (b) the difference between east and west QBO in the 3DO3 run.

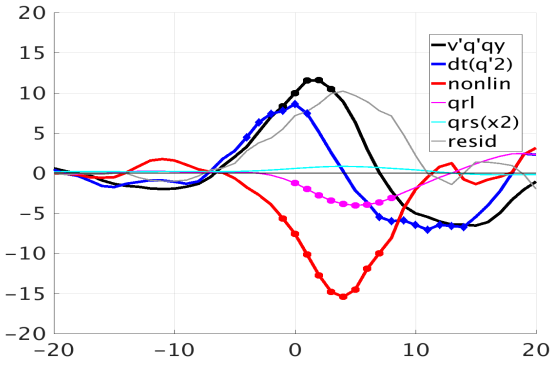

(a) Enstrophy Budget, EQBO

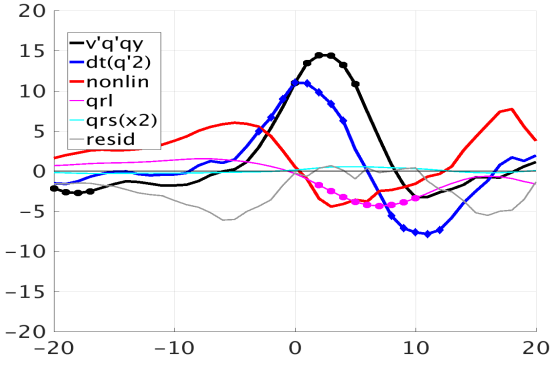

(b) Enstrophy Budget, WQBO

Figure 10. Time lag composit of the enstrophy budget terms ~~normalized by the wave-mean flow term $\overline{v'q'}\overline{q}_y$ at days −3 to 3~~ for east (top), and west (bot) QBO, averaged over 70-40N, 50-0.1mb, for the positive heat flux events from the 3DO3 run of October.

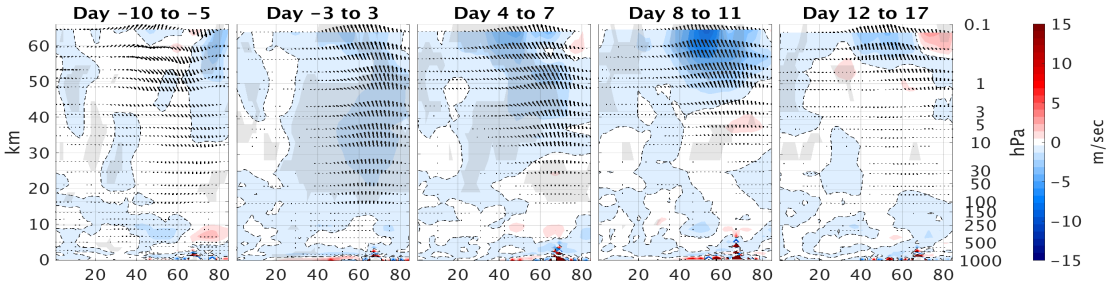

(a) Oct, $\nabla \cdot F$, EQBO ZMO3

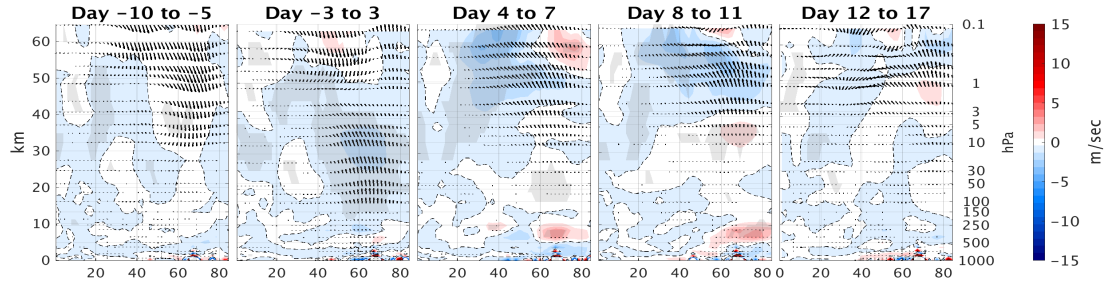

(b) Oct, $\nabla \cdot F$, WQBO ZMO3

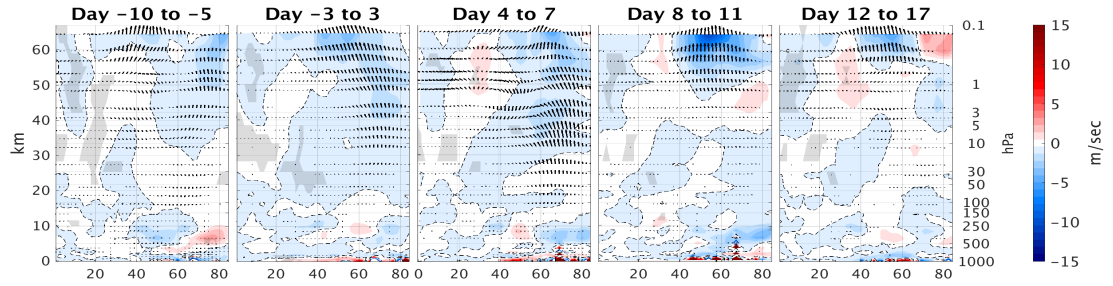

(c) Oct, $\nabla \cdot F$, (E-W)QBO ZMO3

Figure 11. Lat-height time lag ~~composits~~ composites of ~~EP-flux~~ EP flux divergence anomalies from the climatology) for the positive heat flux EQBO (top), WQBO (min), and the difference between them (bot), for October events (70th percentile of $\overline{V'T'}$ at 100mb 85-45N) of the ZMO3 run. Statistically significant areas are shown by gray shading.

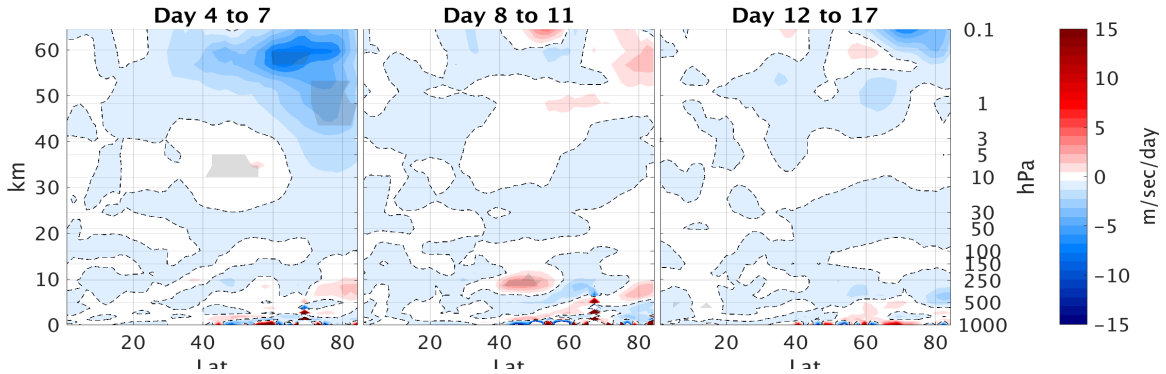

(a) $\nabla \cdot F$, EQBO, 3D-ZM

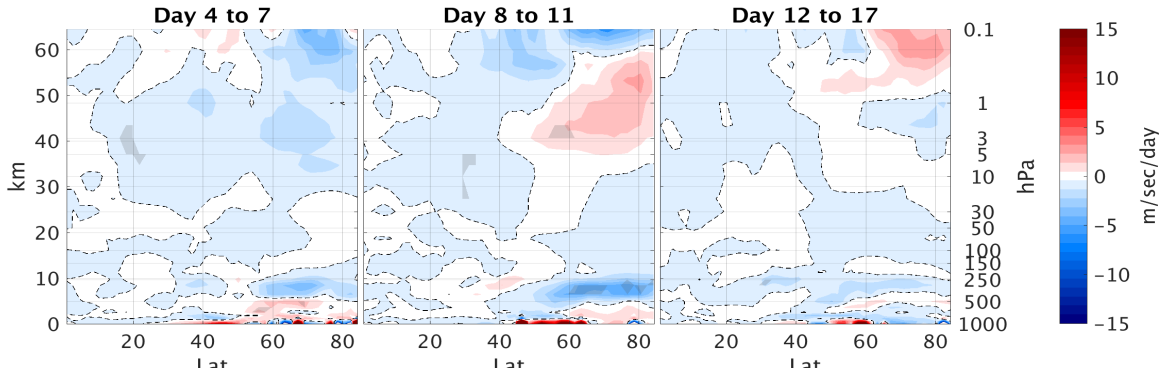

(b) $\nabla \cdot F$, WQBO, 3D-ZM

Figure 12. Lat-height time lag ~~composits~~ composites differences of the 3DO3 and ZMO3 runs of the ~~EP-flux~~ EP flux divergence (colors) ~~and Fzz (contours)~~ for east QBO years (12a) ~~,~~ and ~~the EP-flux divergence (colors) and Fyy (contours) for~~ west QBO years (12b), for October events (70th percentile of $\overline{V'T'}$ at 100mb 85-45N). Dashed contours indicate negative values. Statistically significant areas are shown by gray shading.

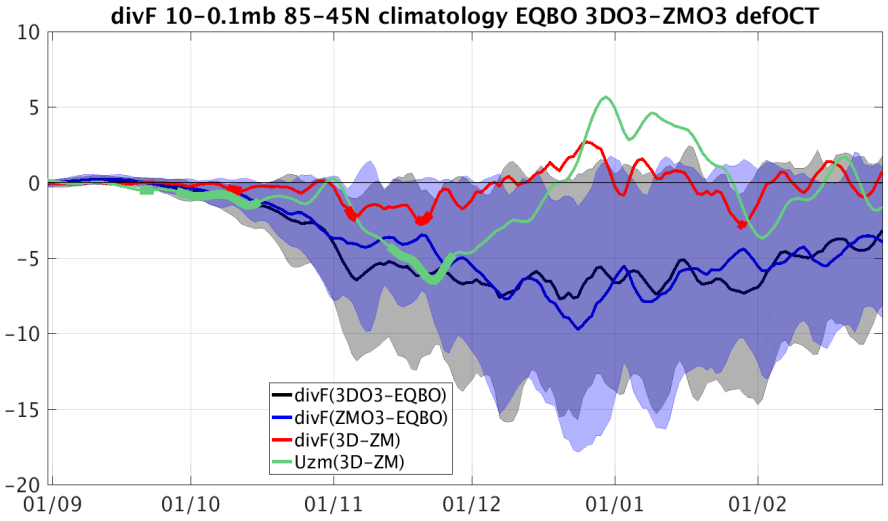

(a) $\nabla \cdot F$, and $\overline{U}$, EQBO, (3D-ZM)

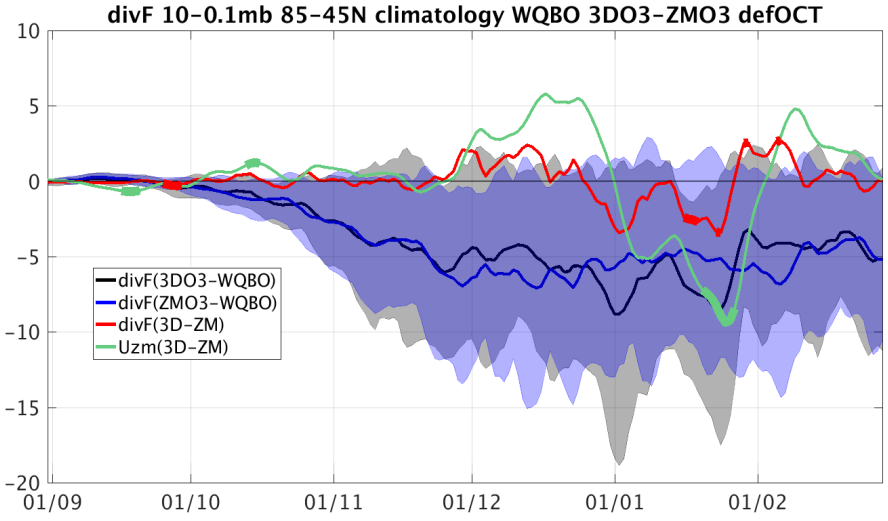

(b) $\nabla \cdot F$, and $\overline{U}$, WQBO, (3D-ZM)

Figure 13. Daily climatology of EQBO (top) and WQBO (bot) years (defined by October) averaged over 10-0.1mb, 85-45N. The ~~EP-flux~~ EP flux divergence for 3DO3 run (black), for ZMO3 run (blue) and their difference (red), with the difference between 3D and ZM runs of the zonal mean zonal wind in green. Gray and Blue shading indicated ± 1 standard deviation from the mean of the 3DO3 and ZMO3 runs correspondingly. Statistical significance is indicated by a thick line.

Appendix A: Appendix

A1 Statistical significance of Figure 4

To calculate the statistical significance of the difference between these to figures we need to have any realizations of each model run. Since this is not possible, we do the following:

1. We take all years of the two simulations, a total of 200 years.
2. Choose randomly a set for two groups of years according to the number of east/west QBO years in each run (two groups for 3DO3 and two for the ZMO3 run).
3. We then average each group and take the difference between then as an east-west mean for each simulation.
4. We repeat this for 1000 times.

We now have 1000 differences of random years for each run. Statistical significance of the 3D(E-W) and ZM(E-W) is calculated similarly but checking if the difference of the E-W (3D-ZM) is bigger/smaller than the 97.5/2.5 percentile of the difference between the two distributions we got.

The result of this calculation is shown in Figure A1 for the zonal mean zonal wind (top) and zonal mean temperature (bot). In the zonal mean zonal winds the negative/positive values in early/late winter indicate that the E-W difference in the 3DO3 run is stronger/weaker than the E-W difference in the ZMO3 run, corresponding to a delay in the HT signal. The differences are statistically significant. The delayed HT signal in the zonal mean temperature is statistically significant as well.

A2 Estimating the direct ozone effect (wave 1 amplitude tendencies)

We focus on zonal wave number 1 since it is the most dominant in the stratosphere. The main balance of temperature time tendency is given by:

$$\frac{dT}{dt} = \frac{dT}{dt}_{dynamics} + \frac{dT}{dt}_{shortwave} + \frac{dT}{dt}_{longwave} \tag{A1}$$

For the zonal wavenumber 1 amplitude balance we use the equations above, apply Fourier transform and take the first wave component. After that we have the following complex terms for temperature wave balance ($s1$ denoting first Fourier component):

$$\widetilde{\frac{dT}{dt}}^{s1} = \widetilde{\frac{dT}{dt}}^{s1}_{dynamics} + \widetilde{\frac{dT}{dt}}^{s1}_{shortwave} + \widetilde{\frac{dT}{dt}}^{s1}_{longwave} \tag{A2}$$

To estimate the time tendency tendency of the temperature wave amplitude from each term in each time step we use the following procedure:

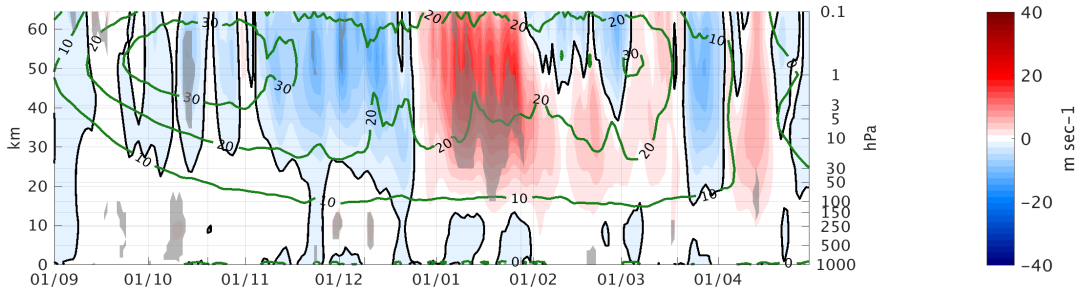

(a) U_{zm}, (E-W)QBO 3DO3-ZMO3

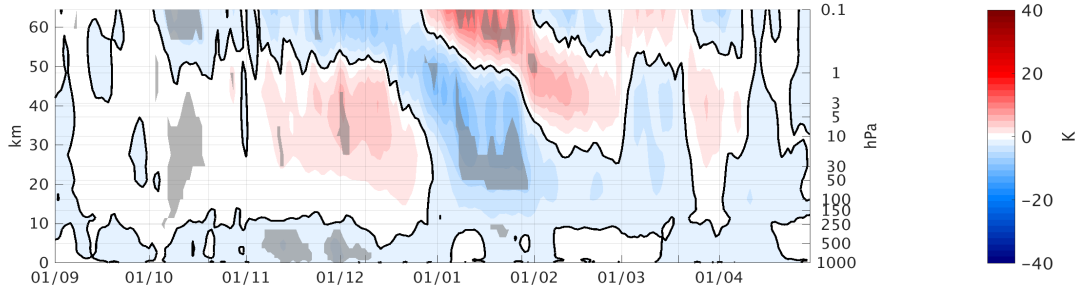

(b) T_{zm}, (E-W)QBO 3DO3-ZMO3

Figure A1. Daily climatology east-west QBO differences between the 3DO3 and ZMO3 model runs of the zonal mean zonal wind averaged over 75-55N (top) and the zonal mean temperature averaged over 90-66N for the 3DO3 (bot), for Sep-Mar. Statistically significant areas are shown by gray shading.

1. Calculate the complex of the next time step from each term: $\widetilde{X}^{j+1}_{term} = \widetilde{X}^{j} + \widetilde{\frac{dT}{dt}}^{j}_{term}$, where "term" is either advection (total or one component), residual, or each of the tendencies from the model/reanalysis.

2. Calculate the change in amplitude: $D^{j}_{term} = |\widetilde{X}^{j+1}_{term}| - |\widetilde{X}^{j}|$, where D^{j}_{term} is the amplitude tendency from a specific term.

It is important to note that this calculation implies the amplitude tendencies from each term do not add up to the total time tendency, however it represents best how each process "attempts" to the change the wave amplitude.

A3 Radiative ozone wave effects on the atmospheric circulation during Summer

In sections 3.1-3.2 we showed the direct radiative effect of ozone waves on the circulation during September. Here we examine the differences between 3DO3 and ZMO3 runs during summer to verify that the September anomalies are not simply carried over from Summer. In particular, an examination of the 3DO3 minus ZMO3 zonal mean short wave heating during summer

(Fig. A1c) reveals a thin band of stronger heating in the 3DO3 run, right at the levels where the model changes back to using 3D ozone in the radiation code in the upper stratosphere which persists into fall. Though this region is significantly reduced to a very small latitude range in early winter (less than 5 degrees in the subtropical region), we need to verify that it is not the source of differences between the 3DO3 and ZMO3 fields during fall and winter.

We find a few indications that this is not the case. First, looking at the zonal mean temperature, and the contribution of dynamics to the temperature time tendency, we find small but significant differences in the zonal mean temperature (Fig. A1a). The polar stratosphere is warmer above 20hPa and colder below in the 3DO3 run during May-Aug by about $1K$. Similar differences are found in Gillett et al. (2009) (Fig. 3d). These differences are dynamically driven as indicated by the zonal mean temperature time tendency from dynamics (Fig. A1b). It is possible however, that the source of differences in the dynamical time tendencies is this anomalous band of short wave heating. Fig. A2) shows the 3DO3-ZMO3 differences of different terms in the zonal mean zonal wind time tendency equation. The zonal mean zonal wind of the 3DO3 run is more westerly in the subtropical lower stratosphere in July, extending upward and poleward until August (Fig. A2a). There is a vertical displacement of the ~~EP-flux~~ EP flux convergence height, with decreased convergence in the lower stratosphere and increased convergence above 30mb (Fig. A2b), well below the region of negative ozone-temperature correlation (indicated by the gray line in the figures). This demonstrates that the vertical displacement of the convergence region is due to the waves reaching higher due to their stronger amplitudes. The total time tendency and the related zonal mean zonal wind anomalies are governed by these changes only during Aug-Sep. Earlier in summer, the time tendency is controlled by the tendency from the Coriolis torque term ($f\bar{v}^*$) above 30mb (Fig. A2c) and by the ~~EP-flux~~ EP flux convergence below.

Finally, in addition to the runs described in this paper, we conducted four 40-year time slice experiments, for which we specified constant east or west QBO phases, for 3DO3 and ZMO3. While the summer heating bands also appeared during summer in these runs, the differences in the Holton-Tan effect between 3DO3 and ZMO3 runs during fall and winter were not found. An examination of October upward wave pulses showed that in both runs there is a stronger EP flux divergence during the late stages of the wave life cycles in west compared to the east QBO phases, but this acceleration is due to nonlinear wave-mean flow interactions rather than to a linear trailing edge acceleration. Correspondingly, the waves are stronger at 100mb in the time slice experiments during October (we are still examining the reasons for these differences). Nonetheless, this suggests that summer heating band is not the source of differences between the 3DO3 and ZMO3 runs found in fall and winter in our time-varying QBO 100-year experiments.

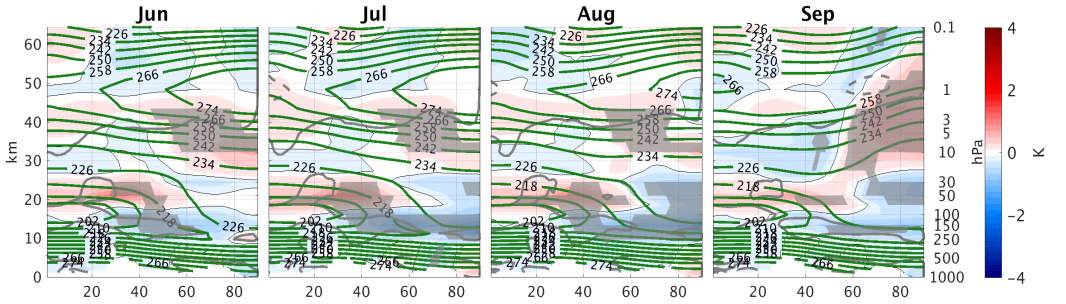

(a) Tzm, 3D-ZM

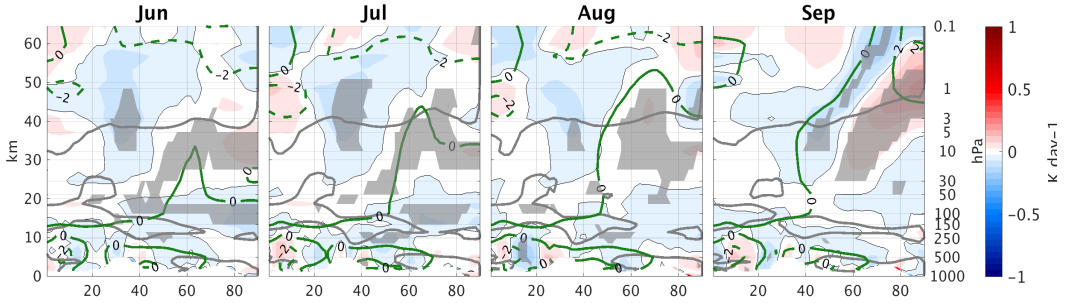

(b) DTCORE, 3D-ZM

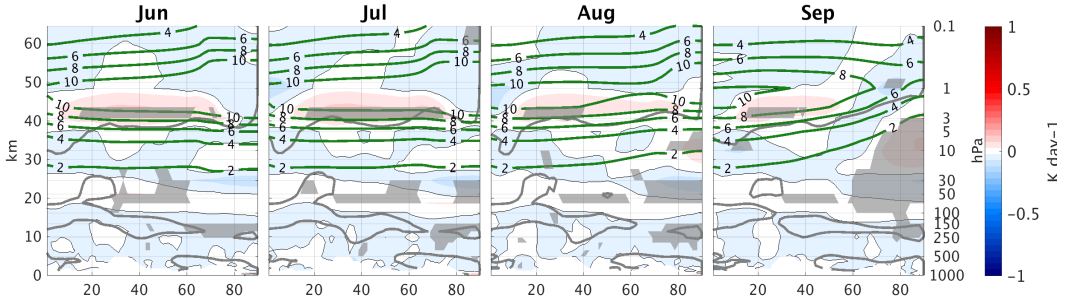

(c) QRSTOT, 3D-ZM

Figure A1. Monthly climatology differences between 3D and ZM ozone runs during summer, Jun-Sep of the zonal mean temperature (A1a), zonal mean temperature tendency from dynamics (A1b), and short-wave radiation (A1c). Statistically significant areas are shown by gray shading.

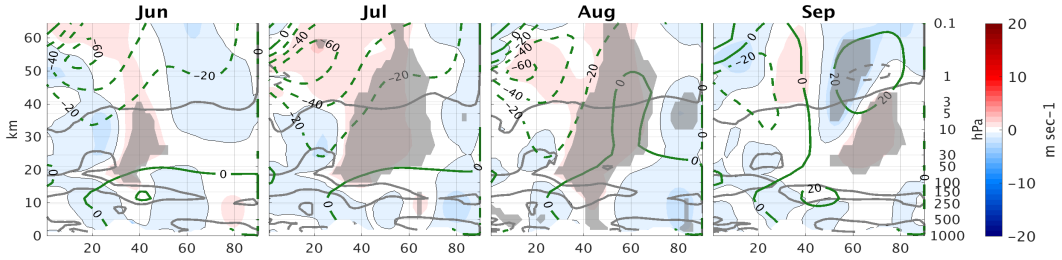

(a) $\overline{U}$, 3D-ZM

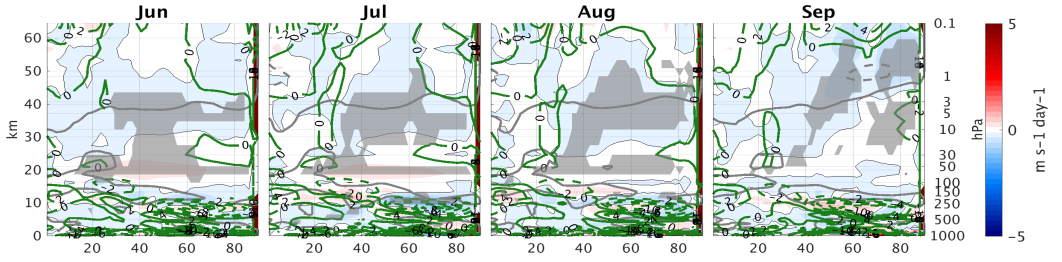

(b) $\nabla \cdot F$, 3D-ZM

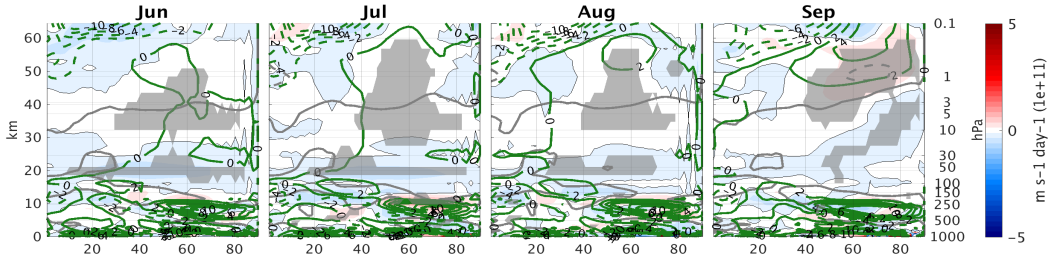

(c) $f\overline{v}^*$, 3D-ZM

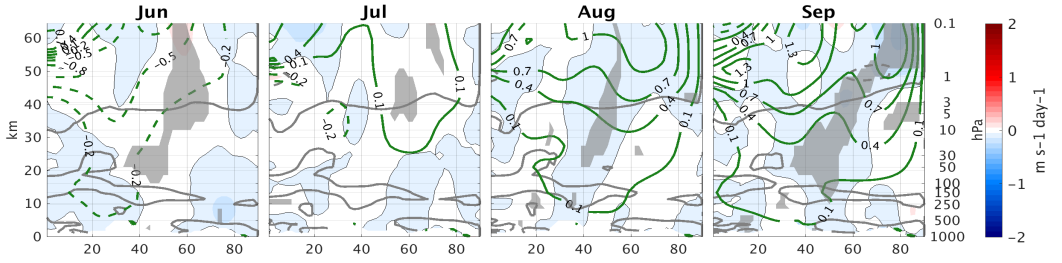

(d) $\frac{d\overline{U}}{dt}$ 3D-ZM

Figure A2. Monthly climatology differences between 3D and ZM ozone runs during summer, Jun-Sep of the zonal mean zonal wind (A2a), zonal mean zonal wind tendency from ~~EP-flux~~ EP flux convergence (A2b), the time ternency from the Coriolis term (A2c), and the total time tendency (A2d). Statistically significant areas are shown by gray shading.

Acknowledgements. We wish to thank the anonymous reviewers for their useful comments. We also wish to thank Chaim Garfinkel for our fruitful discussions.

This work is supported by the German-Israeli Foundation for Scientific Research and Development under grant GIF1151-83.8/2011, and by the Israel Science Foundation (Grant 1537/12). This work has also been partially performed within the Helmholtz University Young Investigators Group NATHAN funded by the Helmholtz Association through the Presidents Initiative and Networking Fund and the GEOMAR Helmholtz Centre for Ocean Research Kiel, Germany. The model simulations were performed at the German Climate Computing Centre (Deutsches Klimarechenzentrum, DKRZ) in Hamburg, Germany.

Part of the work of Nili Harnik was done while on sabbatical at Stockholm University, and supported by a Rossby Visiting Fellowship from the International Meteorological Institute of Stockholm.

We also acknowledge GOAT (Geophysical Observation Analysis Tool; http://www.goat-geo.org) for the data storage organization.

We acknowledge the Israeli Atmospheric and Climatic Data Centre, supported by the Israeli Ministry of Science, Technology and Space, for assisting with the data handling.

References

Albers, J. R. and Nathan, T. R.: Pathways for communicating the effects of stratospheric ozone to the polar vortex: Role of zonally asymmetric ozone, Journal of the Atmospheric Sciences, 69, 785–801, 2012.

Albers, J. R., McCormack, J. P., and Nathan, T. R.: Stratospheric ozone and the morphology of the northern hemisphere planetary waveguide, Journal of Geophysical Research: Atmospheres, 118, 563–576, 2013.

Andrews, D. G., Holton, J. R., and Leovy, C. B.: Middle atmosphere dynamics, 40, Academic press, 1987.

Anstey, J. A. and Shepherd, T. G.: High-latitude influence of the quasi-biennial oscillation, Quarterly Journal of the Royal Meteorological Society, 140, 1–21, 2014.

CCMVal, S.: SPARC Report on the Evaluation of Chemistry-Climate Models, edited by: Eyring, V., Shepherd, TG, and Waugh, DW, Tech. rep., SPARC Report, 2010.

Craig, R. A. and Ohring, G.: The temperature dependence of ozone radiational heating rates in the vicinity of the mesopeak, Journal of Meteorology, 15, 59–62, 1958.

Crook, J., Gillett, N., and Keeley, S.: Sensitivity of Sounthern Hemisphere climate to zonal asymmetry in ozone, Geophys. Res. Lett., 32, 2008.

Douglass, A., Rood, R., and Stolarski, R.: Interpretation of ozone temperature correlations. II-Analysis of SBUV ozone data.[Solar Backscattered Ultraviolet, 1985a.

Douglass, A. R., Rood, R. B., and Stolarski, R. S.: Interpretation of ozone temperature correlations: 2. Analysis of SBUV ozone data, Journal of Geophysical Research: Atmospheres, 90, 10 693–10 708, 1985b.

Eyring, V., Bony, S., Meehl, G. A., Senior, C. A., Stevens, B., Stouffer, R. J., and Taylor, K. E.: Overview of the Coupled Model Intercomparison Project Phase 6 (CMIP6) experimental design and organization, Geoscientific Model Development, 9, 1937–1958, 2016.

Gabriel, A., Peters, D., Krichner, I., and Graf, H.: Effect of zonally asymmetric ozone on stratospheric temperature and planetary wave propagation, Geophys. Res. Lett., 34, 2007.

Garfinkel, C., Silverman, V., Harnik, N., Haspel, C., and Riz, Y.: Stratospheric response to intraseasonal changes in incoming solar radiation, Journal of Geophysical Research: Atmospheres, 120, 7648–7660, 2015.

Garfinkel, C. I., Shaw, T. A., Hartmann, D. L., and Waugh, D. W.: Does the Holton-Tan mechanism explain how the quasi-biennial oscillation modulates the arctic polar vortex?, Journal of the Atmospheric Sciences, 69, 1713–1733, 2012.

Gent, P. R., Danabasoglu, G., Donner, L. J., Holland, M. M., Hunke, E. C., Jayne, S. R., Lawrence, D. M., Neale, R. B., Rasch, P. J., Vertenstein, M., et al.: The community climate system model version 4, Journal of Climate, 24, 4973–4991, 2011.

Gillett, N., Scinocca, J., Plummer, D., and Reader, M.: Sensitivity of climate to dynamically-consistent zonal asymmetries in ozone, Geophys. Res. Lett., 36, 2009.

Gray, L., Phipps, S., Dunkerton, T., Baldwin, M., Drysdale, E., and Allen, M.: A data study of the influence of the equatorial upper stratosphere on Northern-Hemisphere stratospheric sudden warmings, Quarterly Journal of the Royal Meteorological Society, 127, 1985–2003, 2001.

Harnik, N. and Lindzen, R. S.: The effect of reflecting surfaces on the vertical structure and variability of stratospheric planetary waves, Journal of the atmospheric sciences, 58, 2872–2894, 2001.

Hartmann, D.: Some aspects of the coupling between radiation, chemistry, and dynamics in the stratosphere, J. Geophys. Res., 86, 9631–9640, 1981.

Hartmann, D. and Garcia, R.: A Mechanistic Model of Ozone Transport by Planetary Waves in the Stratosphere, J. Atmos. Sci., 36, 350–364, 1979.

Holton, J. and Mass, C.: Stratospheric Vacillation Cycles, J. Atmos. Sci., 33, 2218–2225, 1976.

Holton, J. R. and Tan, H.-C.: The influence of the equatorial quasi-biennial oscillation on the global circulation at 50 mb, Journal of the Atmospheric Sciences, 37, 2200–2208, 1980.

Kodera, K. and Kuroda, Y.: Dynamical response to the solar cycle, Journal of Geophysical Research: Atmospheres, 107, 2002.

Kuroda, Y. and Kodera, K.: Variability of the polar night jet in the Northern and Southern Hemispheres, Journal of Geophysical Research: Atmospheres, 106, 20 703–20 713, 2001.

Labitzke, K. and Van Loon, H.: Associations between the 11-year solar cycle, the QBO and the atmosphere. Part I: the troposphere and stratosphere in the northern hemisphere in winter, Journal of Atmospheric and Terrestrial Physics, 50, 197–206, 1988.

Labitzke, K. and Van Loon, H.: On the association between the QBO and the extratropical stratosphere, Journal of atmospheric and terrestrial physics, 54, 1453–1463, 1992.

Labitzke, K., Kunze, M., and Brönnimann, S.: Sunspots, the QBO and the stratosphere in the North Polar Region–20 years later, Meteorologische Zeitschrift, 15, 355–363, 2006.

Lean, J., Rottman, G., Harder, J., and Kopp, G.: SORCE contributions to new understanding of global change and solar variability, in: The Solar Radiation and Climate Experiment (SORCE), pp. 27–53, Springer, 2005.

Marsh, D. R., Mills, M. J., Kinnison, D. E., Lamarque, J.-F., Calvo, N., and Polvani, L. M.: Climate change from 1850 to 2005 simulated in CESM1 (WACCM), Journal of climate, 26, 7372–7391, 2013.

Matthes, K., Marsh, D. R., Garcia, R. R., Kinnison, D. E., Sassi, F., and Walters, S.: Role of the QBO in modulating the influence of the 11 year solar cycle on the atmosphere using constant forcings, Journal of Geophysical Research: Atmospheres, 115, 2010.

McCormack, J., Nathan, T., and Cordero, E.: The effect of zonally asymmetric ozone heating on the Northern Hemisphere winter polar stratosphere, Geophys. Res. Lett., 38, 2009.

McIntyre, M. E.: How well do we understand the dynamics of stratospheric warmings?, Journal of the Meteorological Society of Japan. Ser. II, 60, 37–65, 1982.

Nathan, T. R. and Cordero, E. C.: An ozone-modified refractive index for vertically propagating planetary waves, Journal of Geophysical Research: Atmospheres, 112, 2007.

Nathan, T. R. and Li, L.: Linear stability of free planetary waves in the presence of radiative–photochemical feedbacks, Journal of the atmospheric sciences, 48, 1837–1855, 1991.

Peters, D. H., Schneidereit, A., Bügelmayer, M., Zülicke, C., and Kirchner, I.: Atmospheric circulation changes in response to an observed stratospheric zonal ozone anomaly, Atmosphere-Ocean, 53, 74–88, 2015.

Ruzmaikin, A., Feynman, J., Jiang, X., and Yung, Y.: Extratropical signature of the quasi-biennial oscillation, J. Geophys. Res, 110, D11 111, 2005.

Scaife, A. A., Athanassiadou, M., Andrews, M., Arribas, A., Baldwin, M., Dunstone, N., Knight, J., MacLachlan, C., Manzini, E., Müller, W. A., et al.: Predictability of the quasi-biennial oscillation and its northern winter teleconnection on seasonal to decadal timescales, Geophysical Research Letters, 41, 1752–1758, 2014.

Scinocca, J., McFarlane, N., Lazare, M., Li, J., and Plummer, D.: Technical Note: The CCCma third generation AGCM and its extension into the middle atmosphere, Atmospheric Chemistry and Physics, 8, 7055–7074, 2008.

Smith, A. K.: Observation of wave-wave interactions in the stratosphere, Journal of the atmospheric sciences, 40, 2484–2496, 1983.

Smith, D. M., Scaife, A. A., Eade, R., and Knight, J. R.: Seasonal to decadal prediction of the winter North Atlantic Oscillation: emerging capability and future prospects, Quarterly Journal of the Royal Meteorological Society, 142, 611–617, 2016.

Taylor, K. E., Stouffer, R. J., and Meehl, G. A.: An overview of CMIP5 and the experiment design, Bulletin of the American Meteorological Society, 93, 485–498, 2012.

Watson, P. A. and Gray, L. J.: How does the quasi-biennial oscillation affect the stratospheric polar vortex?, Journal of the Atmospheric Sciences, 71, 391–409, 2014.

White, I. P., Lu, H., and Mitchell, N. J.: Seasonal evolution of the QBO-induced wave forcing and circulation anomalies in the northern winter stratosphere, Journal of Geophysical Research: Atmospheres, 121, 2016.